Published in final edited form as:

Wiley Interdiscip Rev Nanomed Nanobiotechnol. 2023 ; 15(4): e1889. doi:10.1002/wnan.1889.

Polymer nanomaterials for use as adjuvant surgical tools

Metecan Erdi,

Department of Chemical and Biomolecular Engineering, University of Maryland, 4418 Stadium Dr., College Park, MD 20742, USA

Anthony Sandler,

Sheikh Zayed Institute for Pediatric Surgical Innovation, Joseph E. Robert Jr. Center for Surgical Care, Children's National Medical Center, 111 Michigan Avenue, NW Washington, DC 20010, USA

Peter Kofinas

Department of Chemical and Biomolecular Engineering, University of Maryland, 4418 Stadium Dr., College Park, MD 20742, USA

Abstract

Materials employed in the treatment of conditions encountered in surgical and clinical practice frequently face barriers in translation to application. Shortcomings can be generalized through their reduced mechanical stability, difficulty in handling, and inability to conform or adhere to complex tissue surfaces. To overcome an amalgam of challenges, research has sought utilization of polymer-derived nanomaterials deposited in various fashions and formulations to improve application and outcomes of surgical and clinical interventions. Clinically prevalent applications include topical wound dressings, tissue adhesives, surgical sealants, hemostats, and adhesion barriers, all of which have displayed potential to act as superior alternatives to current materials used in surgical procedures. In this review, emphasis will be placed not only on applications, but also on various design strategies employed in fabrication. This review is designed to provide a broad and thought-provoking understanding of nanomaterials as adjuvant tools for assisted treatment of pathologies prevalent in surgery.

Graphical Abstract

Current materials deployed in surgery as wound dressings, tissue adhesives, surgical sealants, hemostats, and post-operative adhesion barriers are prone to failure due to a non-optimized balance of cohesive and adhesive strength.

kofinas@umd.edu .

Conflict of Interest

The authors have no conflicts of interest.

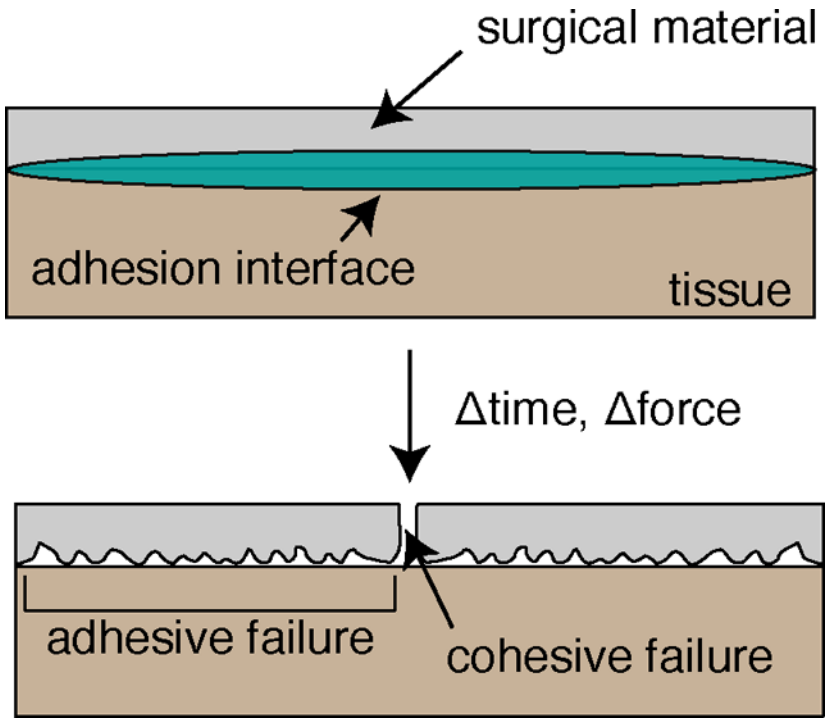

1. INTRODUCTION

Conventional materials deployed in surgery for improved treatment of clinical pathologies suffer from a combination of inferior mechanical properties, difficult handling, and poor biocompatibility. These material shortcomings lead to decreased treatment efficacy and poor patient outcomes in wound dressings (Figure 1A), tissue adhesives (Figure 1B), surgical sealants (Figure 1C), hemostats (Figure 1D), and post-operative adhesion barriers (Figure 1E). Such materials were chosen as the focus for this review due to a combination of their impact in clinical operations and high frequency of recently published research investigations.

Novel research nanomaterial approaches in the treatment of multiple clinical conditions are often polymer fibers or swellable polymer networks. Preclinical use of solution blow spinning as a means for deposition of fibers through pressure driven airbrush flow of a polymer solution has been developed in the Medeiros, Kofinas, and Sandler research groups. (Daristotle et al., 2016; Medeiros et al., 2009) This potentially allows for simple deposition of polymer fiber mats with nanoscale diameter (80 – 1000nm) and porosities (~1000nm) for a multitude of surgical applications (Figure 2A). Electrospinning is an additional method for deposition of similar nanoscale fibers (90 – 1000nm diameter), which in contrast to a simple airbrush setup, necessitates an electrically conductive substrate, an electric field with polarizing current, 10 times slower deposition times, and dissolution of polymer in toxic solvent (Figure 2B).(Greiner & Wendorff, 2007; Medeiros et al., 2009; Polat et al., 2016; Tutak et al., 2013). Hydrogels are polymer networks with nanometer scale pores (~100nm) that swell with water in aqueous environments within tissue, thereby preventing dehydration and accelerating the rate of fibrogenesis and angiogenesis (Figure 2C).(Junker et al., 2013)

Sealing of a tissue site via a hydrogel also presents a diffusion limitation to external pathogen transport to site of injury, thereby reducing risk of infection as compared to dry materials.(Field & Kerstein, 1994; Singh et al., 2004) However, hydrogel-based systems present subpar mechanical behavior. They are usually brittle and tend to swell rapidly when excess fluid is present. Fabrication complexities highlight further translational barriers of applying hydrogels in surgery, such as 1) requiring a dual barrel syringe injection approach in which pre-polymer solution is mixed at a tip with a crosslinking initiator or 2) benchtop solution casting and molding for a specific clinical application. This review will compile research on nanomaterials utilized in combating the shortcomings of clinical, tissue adhesive materials used in surgery, while also highlighting their respective modes of application.

2. WOUND DRESSINGS

Wounds from burns or trauma account for approximately 1.2 million hospital admissions each year, with resultant infections presenting a 75% risk of mortality if left untreated. (Church et al., 2006) The high mortality and infection rates underscore the inability of current materials to facilitate biocompatible and effective wound healing, as they fail to create the ideal environment sealed off from potential infectious agents and fluid loss. Examples of prefabricated poly(urethane) film (Tegaderm) and poly(urethane) foam (Mepilex) dressings frequently deployed in wound care are coated with an acrylic adhesive layer that is non-degradable, and thereby cannot remain indefinitely at the point of application. Both materials are non-conformal to nanoscale tissue topography, irregular in shape and depth, and frequently detach from their applied substrate. This necessitates either repeated dressing replacements that disrupt the continuous wound healing process or additional modes of fixation to tissue. Hence, a combination of non-degradability and subpar mechanical properties in current commercial dressings implores exploration of novel research materials. Clinically relevant materials will be ones with an optimized balance between biodegradation rate, epidermal tissue adherence, and mode of administration (Tables 1–2).

Translationally effective wound dressings should be inherently robust, yet flexible and adhesive, and contain materials with rapid deposition times to the site of injury *in situ*. This milieu of properties aids in the promotion of angio- and fibro- genesis in wound models of various depths. A common and relevant metric studied in wound healing is the measurement of epidermal wound closure assessed either through top-down images of wounds or histological cross sections sampled over a clinical time course (Figure 1A).

Blowspun burn wound dressings developed by Behrens et al. and Daristotle et al. deposited a blend of poly(lactic-co-glycolic acid) and poly(ethylene glycol), that upon warming up to body temperature at 37°C, induces adhesion to epidermal tissue due to melting of the poly(ethylene glycol) plasticizer within the poly(lactic-co-glycolic acid) matrix.(Behrens et al., 2015; Daristotle, Lau, et al., 2020) An additional application by Daristotle et al. employed the same technology in a viscoelastic blend of poly(lactide-co-caprolactone) as to create a biocompatible band-aid adhesive with pressure dependent adhesive properties. (Daristotle et al., 2021) Prefabricated electrospun fiber mats are a popular dressing medium due to the porous and rigid structure of the resultant nanomaterial. Ahmed et al. explored

electrospun chitosan-poly(vinyl alcohol)-zinc oxide fibers in a rabbit model, displaying marked success in epidermal skin wound closure versus clinical control.(Ahmed et al., 2018) This is due in large part to the presence of chitosan, a naturally occurring biopolymer that harbors great biocompatibility, antimicrobial properties, and ability to facilitate fibroblast proliferation as a result of biodegradation products. While these technologies employ mechanisms of biocompatible, non-toxic adhesive curing and porous fiber mats allowing for oxygen permeation, both classes of nanofiber mats could benefit from an aqueous environment native to tissue.(Amiri et al., 2020; Dunn et al., 2016; Ju et al., 2016; Xie et al., 2013; K. Zhang et al., 2021; Zhao, Sun, et al., 2017)

While the inability for rapid, in situ fabricated, hydrogel-derived, dressing material presents a practical disadvantage, such systems are a popular research material as wound healing mediums due to an aqueous environment adept to wound healing. He at al. explored use of an amino acid-derived inhibitor of nitric oxide to lower the inflammatory response and promote collagen regeneration.(M. He et al., 2019) Although this presents a promising biological pathway to improving wound healing efficacy, such a material is notably prefabricated and requires a secondary, clinical polyurethane control (Tegaderm) to secure it at the site of injury and facilitate a critical moist environment. Wang et al. also embodies a similar, therapeutic approach through loading of chitosan microspheres with poly(pyrrole) and rose bengal — a staining compound explored as a treatment for skin conditions — as to promote recruitment of angiogenic growth factors and antibacterial activity.(J. Wang et al., 2021) Wu et al. loaded an anti-inflammatory agent in curcumin into a poly(vinyl alcohol) and glycerol as to form an organohydrogel with non-drying behavior.(Wu et al., 2023) Translation concerns are highlighted not only through their complex manufacturing technique, but also the necessity of an additional visible light and near infrared light curing step as to induce anti-bacterial activity of loaded compounds in select scenarios. With inspiration derived from underwater mussel foot protein adhesion, dopamine containing hydrogels present a novel bioinspired pathway to improving tissue adhesion and retention at the site of application for wound healing materials. While dopamine does encourage nanoscale, non-covalent interactions with substrates, its binding interaction is intrinsically rigid on its own and thereby necessitates blending of additional support structures such as those explored by Huang et al., Han et al., and others.(T. Chen et al., 2018; GhavamiNejad et al., 2016; Han et al., 2016; Han, Yan, et al., 2017; Y. Huang et al., 2020; Liang, Zhao, Hu, Han, et al., 2019; Ryu et al., 2018; L. Wang et al., 2020; K. Zhang et al., 2021; Zhao et al., 2020) Delineation of chemically-derived dopamine adhesion versus physically-derived hydrogel adhesion could be better highlighted to elucidate novelty, while in addition supporting structures with improved flexibility. Several other hydrogel incorporating strategies have been explored, but present lesser success in epidermal skin wound closure versus control than those mentioned.(Blacklow et al., 2019; G. Chen et al., 2018; Gan et al., 2019; Griffin et al., 2015; Guo et al., 2022; J. He et al., 2020; W. Huang et al., 2018; S. Li et al., 2020; Liang et al., 2020; Liang, Zhao, Hu, Chen, et al., 2019; Lokhande et al., 2018; Lu et al., 2017; Ma et al., 2019; Qu et al., 2018; Tang et al., 2020; Turabee et al., 2019; Ying et al., 2019; Zhao, Wu, et al., 2017; Zhu et al., 2018)

3. TISSUE ADHESIVES

Polymeric tissue adhesives currently deployed in surgery include acrylate and poly(ethylene glycol) (PEG) based materials. n-Butyl cyanoacrylate (ex. Histoacryl) and 2-Octyl cyanoacrylate (ex. Dermabond) are commonly employed chemistries of topical adhesives. (Singer, Perry, et al., 2008) These materials are presented as a liquid that polymerize in the presence of water to form a “glue” and adhere to applied tissue substrates.(Singer, Quinn, et al., 2008) Non-degradability of acrylate-based adhesives present toxicity concerns, largely restricting them to topical application on skin, where even then cases of allergic contact dermatitis and stripping of healthy skin during healing are presented.(Deng, 2018; Falsafi et al., 2000; Shin et al., 2011) An additional class of synthetic tissue adhesives constructed with PEG presents a non-toxic and biocompatible alternative to acrylate-based materials. (Nam & Mooney, 2021) However, a high degree of swelling and utilization of ultraviolet light-initiated polymerization to interface with tissue highlight drawbacks of PEG-based tissue adhesives. Coupled with poor cohesive strength, researched tissue adhesives need to explore an approach that optimize a synergy of administration in surgical settings, and mechanical properties of both cohesion and adhesion (Figure 1B).

A candidate tissue adhesive for surgery needs be easily applied, present minimal toxicity concerns, and exhibit a combination of high adhesive strength and cohesive strength as to reduce risk of failure (Tables 3–4). Deposition of tissue adhesive nanofiber mats has been explored by Kofinas and Sandler through solution blow spinning. Behrens et al. and Daristotle et al. devised an inventive method of adhesive curing through simple melting of PEG at body temperature within a PLGA matrix, while Daristotle et al. and Erdi et al. employed polymer viscoelasticity as to create a pressure sensitive tissue adhesive. (Behrens et al., 2015; Daristotle et al., 2021; Daristotle, Zaki, et al., 2020; Erdi et al., 2022) Both are non-toxic adhesive curing approaches employing fundamental material phenomena and present appreciable adhesion to various *ex vivo* tissue surfaces in the range of 10 – 30 kPa. Adhesion to tissue through solely physical interactions — namely short-range, nanoscale Van der Waals and hydrogen bonding — limits the adhesion strength.(Felton, 1997; Kinloch, 1980; Peppas & Buri, 1985) Specific nanoscale chemical interactions rather than macroscopic, physical polymer entanglements with tissue could prove to be an optimal method for generating adhesion.

Hydrogel systems with added chemical moieties designed to interact with functional groups expressed on tissue present an intriguing route to biocompatible tissue adhesion. Bioinspired approaches are highlighted through physical and chemical binding of mussel adhesive proteins to terminal amine and oxygen-containing residues expressed on both internal, mesothelial tissue and external, epidermal tissue.(Y. S. Kim, 1974; Kord Forooshani & Lee, 2017) Han et al. introduced poly(dopamine) nanoparticles into a thermally-reversible, self-healing poly (N-isopropylacrylamide) hydrogel matrix and provided for excellent adhesion to pig skin (~85 kPa).(Han et al., 2016) A multi-step synthesis that includes an additional soaking of their hydrogel in a poly(dopamine) nanoparticle suspension and thereby diminishes the practical value of their material in surgical settings. A patch application studied by Jeon et al. uses a mussel adhesive protein hydrogel coating on silk-based microneedles.(Jeon et al., 2019) While significant adhesion strength is presented on

both dry pig skin (~125 kPa) and pig intestine (~105 kPa), similar concerns are expressed. However, reduced cohesive strength (i.e. brittleness) and specificity of chemical interactions contributing to adhesion is of note in mussel inspired materials.(T. Chen et al., 2018; W. Chen et al., 2017; Fan et al., 2016; Han et al., 2018; Han, Yan, et al., 2017; X. He et al., 2019; M. Li et al., 2020; Liang, Zhao, Hu, Chen, et al., 2019; Liang, Zhao, Hu, Han, et al., 2019; Y. Liu et al., 2014; Pinnaratip et al., 2018; Suneetha et al., 2019; L. Wang et al., 2020; Zhao et al., 2020)

N-hydrosuccinimide (NHS) ester chemistry is a widely employed technique for hydrogel synthesis.(Hermanson, 2013) This is due to simple carbodiimide activation of carboxylate molecules that then readily react with primary amine groups and form stable amide bonds. However, prevalence of amine groups expressed on various tissue also presents an opportunity to couple covalently with an NHS ester functionalized material. Kelmansky et al. (~175 kPa on pig skin) and Zhang et al. (~100 kPa on rat skin) each deploy a singular approach to generating tissue adhesion through use of NHS ester functionalized polymers as injectable glues.(Kelmansky et al., 2017; W. Zhang et al., 2020) Yuk et al. employs a two-factor approach in generating tissue adhesion through grafting of NHS onto poly(acrylic acid) (PAA) in a biopolymer composite hydrogel of gelatin and chitosan supported by a poly(ethylene) backing as to create a “tape-like” material.(Yuk et al., 2019) The studied hydrogel system facilitates rapid hydration and swelling — effectively drying wet tissue surfaces — while also providing for a baseline level of cohesive strength. Reactivity of NHS ester with primary amine groups contained in protein structures on the dried tissue provides for improved adhesive strength. A combination of unique cohesive and adhesive strength inducing mechanisms thereby yields high levels of tissue adhesion (120 kPa / 100 kPa / 100 kPa) on a multitude of ex vivo pig tissue substrates (skin / intestine / aorta). Both glue and complex hydrogel systems generate significantly improved levels of tissue adhesion as compared to previously described neat fiber and hydrogel systems. However, such approaches are not inherently biocompatible or inherently translatable for clinical application. It is known that unreacted carbodiimide used in NHS activation presents concentration-dependent toxicity to collagen scaffolds containing fibroblasts and keratinocytes.(Hanthamrongwit et al., 1996; Powell & Boyce, 2006) Glue systems by Kelmansky et al. and Zhang et al. present diminished levels of cohesive strength critical for extensive, internal in vivo implantation. In the tape system by Yuk et al., an extensive fabrication and application process involving ultraviolet curing of their composite hydrogel, deposition onto a backing layer, storage under desiccation, and sequential peeling of backing layer upon application reduces its clinical translatability. Similar concerns are expressed in other materials approaches deriving tissue adhesion via NHS ester chemistry.(Bu et al., 2019; Sun et al., 2020; H. Zhang et al., 2015)

Other neat and combinatorial hydrogel systems that employ neither bioinspired mussel adhesion nor NHS ester chemistry have been explored, but only present moderate increase in adhesion strength, as some were not necessarily designed to act as an effective tissue adhesive in surgery.(Annabi et al., 2017; Anthis et al., 2021; Assmann et al., 2017; Bai et al., 2019; Du et al., 2020; Hong et al., 2019; H. J. Kim et al., 2015; Lang et al., 2014; J. N. Lee et al., 2021; Y. Lee et al., 2015; Nishiguchi & Taguchi, 2020; Okada et al., 2017; Shirzaei Sani, Kheirkhah, et al., 2019; Shirzaei Sani, Portillo Lara, et al., 2019; Z. Wang et al.,

2021; Zhou et al., 2021) The collection of these nanomaterials similarly present translational barriers of prefabrication, brittle mechanical properties, or toxicity of unreacted hydrogel synthesis components.

4. SURGICAL SEALANTS

Clinically adopted surgical sealants include fibrin (ex. TISSEEL) and PEG based (ex. CoSeal) materials. However, neither formulation is effective in preventing leakage due to a combination of their method of application or weak adhesion to tissue. Fibrin glues are a cocktail of quickly clotting blood proteins (fibrinogen, thrombin, etc.), but are expensive — as components need to be isolated from autologous or donor sources — and are complex to deploy.(Spotnitz, 2010; Spotnitz & Burks, 2012; Wallace et al., 2001) PEG based sealants that employ reactive NHS ester chemistry as to interface with tissue are prevalent in the clinic, but require extensive preparation and present high degrees of swelling leading to injury of surrounding structures. Extraneous sutures and staples are common non-biomaterial approaches in preventing leakage but can be intensive processes that rely upon natural fibrosis to seal off affected segments of tissue (Figure 1C). Such shortcomings have led to research into biocompatible, resourceful, and effective surgical sealant approaches (Tables 5–6).

Polymer nanofiber mats deposited via solution blow spinning (SBS) are a facile method for generating a surgical sealant that overcomes translational barriers of conventional materials. In investigations by the Kofinas and Sandler research groups, Behrens et al. and Kern et al. utilize this technology in creation of a PLGA and PEG composite fiber mat with body temperature mediated adhesion.(Behrens et al., 2015; Kern et al., 2017) Such an approach provides for a combination of adhesive strength via melting of PEG within a cohesive rigid PLGA matrix and thus yields an appreciable burst pressure (~ 9kPa). Further improvements in burst pressure strength via SBS via incorporation of aggregating, hemostatic silica nanoparticles by Daristotle et al. was investigated.(Daristotle et al., 2019) Mechanically rigid nanoparticles improve properties of cohesion, leading to a markedly higher burst pressure (~19 kPa). In a separate investigation, Daristotle et al. studied ratio blends of low and high molecular weight poly(lactide-co-caprolactone) (PLCL).(Daristotle, Zaki, et al., 2020) Adhesive strength and tissue spreadability is induced via liquid-like low molecular weight chains able to form interfacial physical bonds with tissue at the nanoscale, while cohesion strength is provided by solid-like, high molecular weight constituents. Despite being designed to act as a biodegradable tissue adhesive, burst pressure values were the highest here as compared to the group's previous investigations (~40 kPa). Variable ratios and molecular weights could be further explored to increase burst pressure and tune to *in vivo* sealant applications.

Novel hydrogel architectures present a promising pathway for development of surgical sealant nanomaterials. Blending of biocompatible chitosan with a microbial enzyme by Fernandez et al. aims to overcome poor tissue adhesiveness in neat chitosan materials. (Fernandez et al., 2017) While a high burst pressure (~125 kPa) is achieved on a clinically relevant pig intestine, spray deposition of enzyme catalyzed chitosan via a double cannister spray device necessitated a 5-minute adhesive curing period that would not lend itself well to

fast-paced operating conditions. Other chitosan-based sealant systems present a combination of moderate burst pressure due to inherent brittleness of chitosan in addition to clinical translation difficulties.(Du et al., 2020; Ryu et al., 2019) Shirzaei Sani et al. and Zhou et al. both synthesize hydrogels derived from gelatin — a naturally occurring biopolymer in connective tissue — and present moderately high pressures in pig intestine (~60 kPa) and pig skin (~35 kPa), respectively.(Shirzaei Sani, Kheirkhah, et al., 2019; Zhou et al., 2021) The initial system proposed necessities a visible-light adhesive curing of a prepolymer solution containing methacrylic anhydride that if left unreacted reacts exothermally with water. Burst pressure as tested by the authors employs a modified setup with stainless steel plates and air driven flow, similar to that proposed in Figure 1C, and thereby fails to directly mirror aqueous conditions and water driven flow in intestinal systems. The former scheme necessitates a 20-minute self-crosslinking step following injection of prepolymer solution, thereby diminishing clinical applicability. Hong et al. investigates a gelatin-hyaluronic acid derived system that necessitates a toxic, ultraviolet light source for *in situ* gelation at incision site on pig intestine (~40 kPa), while Bu et al. employs use of PEG-NHS ester chemistry that requires a 5-minute gelation period prior to testing and aforementioned concerns of concentration-dependent toxicity and dual-syringe injection.(Bu et al., 2019; Hong et al., 2019) Other gelatin (Assmann et al., 2017; Luo et al., 2019), NHS ester (Kelmansky et al., 2017; Shimony et al., 2021; Sun et al., 2020), and blended hydrogel (Annabi et al., 2017; Anthis et al., 2021; Jeon et al., 2019; Z. Zhang et al., 2018) systems have been studied as surgical sealant materials, yet they present moderate burst pressure values and encounter great concerns stemming from their prefabricated form.

5. HEMOSTATS

Effective hemostatic materials are those that present an ability to absorb blood and prevent blood loss at sites of epithelial tissue injury (laceration, amputation, puncture, etc.) (Figure 1D). Failure of current materials to treat hemorrhage accounts for 33% of all traumatic deaths in controlled clinical settings, whilst also accounting for nearly 90% of deaths in the military sector.(Evans et al., 2010; Kelly et al., 2008) Fibrin based glues (ex. TISSEEL) currently deployed in the clinic are expensive and are often dependent on patient blood composition to induce coagulation, hence their approval namely as adjuncts in surgery. (Spotnitz, 2010) Biologically derived hemostats approved for use in the clinic are frequently biopolymer (ex. Angio-Seal) or protein (ex. ProGel) based hydrogel materials restricted to use in select clinical pathologies.(Deuling et al., 2008; Fuller, 2013) Though effective in certain instances, there exists a need to further improve range of applicability and time-dependent coagulation of hemostatic materials (Tables 7–8).

Early investigations in the Kofinas and Sandler research groups by Behrens et al. and Fathi et al. studied hydrogel particle suspensions of N-(3-aminopropyl)methacrylamide (APM) and zeolite-loaded alginate-chitosan, respectively.(Behrens et al., 2014; Fathi et al., 2018) Both APM and chitosan are charged, cationic materials that aid in the process of hemostasis through activation of the coagulation cascade.(Wang et al., 2019) Hydrogel swellability in both formulations further augments hemostatic properties through formation of a physical, plug-like barrier. While each displays marked success in reducing clotting time in vitro and in vivo, both are prefabricated via inverse suspension polymerization technique, followed by

repeated washing and drying steps, and a 5-minute application process *in vivo*. Deposition of hemostatic material by Daristotle et al. via solution blow spinning counteracts the extensive synthesis process and slow deposition times in both hydrogel particle approaches.(Daristotle et al., 2019) A polymer blend of poly(lactic-co-glycolic acid)/poly(ethylene glycol) with negatively charged silica nanoparticles induces coagulation through a glass effect, whilst also providing for far improved cohesive and adhesive strength via enhanced interfacial interactions with tissue at the nanolevel.(Ostomel et al., 2007) However, only a moderate change in coagulation time is achieved in vivo (~3 min) versus clinical control (~4 min). Additional synthetic hydrogels and liquid suspensions have been explored due to their natural swelling ability and sequential formation of a physical barrier to hemostasis, albeit to lesser success versus clinical control in both low and high impact animal models.(Chan et al., 2015; Du et al., 2020; Hong et al., 2019; Hoque et al., 2017; Hsu et al., 2015; Luo et al., 2019; Mao et al., 2021; Z. Wang et al., 2021)

Bioinspired marine mussel adhesion via binding of catechol-containing proteins to amine and oxygen-containing residues on tissue is a prevalent route for generating hemostasis. Formed nanostructures yield strong adhesion in the presence of water and other aqueous media due to the formation of both chemical and physical bonds with substrates.(Han, Lu, et al., 2017) Hence, materials containing catecholic structures (ex: dopamine) provide a pathway to reducing failure of materials in which excess blood is present. Li et al. incorporates poly(dopamine) into naturally hemostatic chitosan as to form a cryogel (i.e. lyophilized hydrogel).(M. Li et al., 2020) Though the material presents ubiquitous applicability to act as a hemostat through testing in various animal models, the extensive prefabrication process and need to use a toxic, strong oxidizing agent ($NaIO_4$) as to generate a poly(dopamine) structure hinders its value in fast-paced surgical settings. Xuan et al. similarly employs use of dopamine-based chemistry in a bilayer nanosheet containing gelatin and poly(caprolactone) (PCL).(Xuan et al., 2020) Gelatin containing dopamine induces hemostatic activity through its combinatorial swelling and wet tissue adhesive properties, while the PCL layer provides for mechanical robustness. A complex spin coating of the gelatin/dopamine layer containing an oxidizing agent ($CaCl_2$), coupled with both plasma and ultraviolet curing steps, lessens excitement for use in the clinic. Bai et al. adopts a more biocompatible approach through combination of a dopamine analogue in tannic acid within a silk protein.(Bai et al., 2019) The authors evidence the ability of natural silk fibers to self-assemble into nanostructures through physical interactions and thus contribute to formation of a physical, plug-like bulk structure critical to hemostasis. Though effectively reduced clotting time (~1 min) is presented in a rat liver puncture model versus control (~5.5 min), reliance upon expensive natural silk production and solely tannic acid-tissue interactions for generating adhesion inhibit clinical scalability. Other catechol containing bioinspired hemostats have been explored but are either less effective in reducing blood flow or present translatability concerns.(C. Liu et al., 2018)

Porous nanostructures within materials present a physical mechanism to hemostasis through rapid uptake of blood. Zhang et al. implements such an approach through an agarose-poly(ethylene glycol) hydrogel with self-healing properties.(Z. Zhang et al., 2018) However, the use of remnant benzaldehyde in the system to generate adhesion with tissue surface proteins presents toxicity concerns, in addition to its involved synthesis and prefabrication.

Synthetic foam sponges such as those made by Lan et al. and Liu et al. accomplish that through chitosan and dextran-based chemistries, respectively.(Lan et al., 2015; C. Liu et al., 2019) The non-biodegradable nature necessitates removal following application at the site of injury, deterring from its use in surgery. Both approaches, in addition to other porous nanomaterials, could also benefit from testing in larger and more intensive animal models as to qualify hemostatic efficacy.(S. Chen et al., 2018; Dowling et al., 2015; Yan et al., 2017; L. Yu et al., 2019; Yuan et al., 2020)

6. ADHESION BARRIERS

Adhesions are rigid, fibrous bands that adjoin tissue surfaces as a result of inflammatory or ischemic conditions following postoperative mesothelial injury (abrasion, ligation, anastomosis, etc.) (Figure 1E). Studies have shown a 93% occurrence rate following abdominal surgery and complications of small bowel obstruction, chronic pelvic pain and female infertility occur, and accounts for over $2 billion in healthcare costs.(Menzies, 1992, 1993; Menzies & Ellis, 1990; Moscowitz & Wexner, 2000) A dried biopolymer, sheet-like film (Seprafilm) currently deployed in surgery is often described by operators as “brittle” and “sticky”, thus rendering it difficult to apply and inconsistent in treatment efficacy. Additional conventional strategies include gel-based materials designed to sustain shear forces imparted by the perpetual shifting of organs *in vivo*, as well as dropwise administration (Icodextrin) of anti-inflammatory and hemostatic therapeutics targeting non-physical pathways.(Catena et al., 2012) Clinical translation of barriers is largely impeded by either their mechanical properties or means of application, while delivery of anti-inflammatory drugs presents issues of controlled release and systemic effects even when topically administered (Tables 9–10).

Deposition of polymer fibers presents a unique method of generating tissue adherent scaffolds for use as solid adhesion barriers. In a recently published collaborative investigation by the Kofinas and Sandler research groups, Erdi et al. spray deposited viscoelastic molecular weight blends of poly(lactide-co-caprolactone) (PLCL) via solution blow spinning.(Erdi et al., 2022) Prevention of high grade, rigid scar tissue formation in a mouse cecal ligation model is achieved through a tuned, surface degradation mechanism preventing prolonged adherences of molecules capable of generating adhesions. An alternative method for fiber generation via electrospinning of poly(ethylene glycol)/poly(caprolactone) by Chen et al. generates nanofibrous membranes to prevent adhesion deposition.(C.-H. Chen et al., 2015) Here, a porous structure allows for nutrient diffusion whilst inhibiting fibroblast penetration and proliferation yields significantly reduced adhesion severity in a rabbit tendon anastomosis model. Utility of fibrous and electrospun materials in surgical settings, such as long deposition times and a complex setup requiring a conductive substrate in vitro, diminishes their value in operational conditions.(Leberfinger et al., 2018; Xia et al., 2015)

Hydrogel based materials aim to prevent adhesion via hydrophilic and lubricious surface properties at the material-tissue interface that inhibit the prolonged adherence of fibro- and angio- genic molecules. Stapleton et al. synthesizes a physical hydrogel through incorporation of poly(ethylene glycol)-b-poly(lactic acid) nanoparticles within

a hydrophobically modified cellulose matrix.(Stapleton et al., 2019, 2021) Traditional hydrogel systems achieve gelation through formation of chemical, static crosslinks via use of a toxic initiator. Here, the authors employ non-covalent entropic and hydrogen bonding nanoscale interactions between particle and hydrogel as to form dynamic crosslinks in a biocompatible manner. Though reduction of scored scar tissue severity is achieved in two separate rat animal models, it is important to consider the brittle and swellable nature of hydrogels once formed. Song et al. alternatively introduces hemostatic chitosan within a hyaluronic acid hydrogel matrix as to induce significant reduction of severe adhesions in a rat abdominal wall abrasion model.(Song et al., 2016) The authors here employ a strong oxidizer ($NaIO_4$) and strong acid ($ClCH_2COOH$) in synthesis of each individual component, whilst also taking 66 seconds to fully gelate following subcutaneous injection. In hydrogel focused work by Stapleton et al., Song et al, and others, there exists a potential to fail if injured tissue at the site of application flexes too greatly or is in a confined space with other organs in its proximity that may experience undue pressure. Other neat hydrogel approaches have been studied but are frequented with either toxic initiators for gelation or do not study high impact models for adhesion formation.(Bang et al., 2016; Cai et al., 2018; C.-H. Chen et al., 2017; Z. Li et al., 2020; Mayes et al., 2020; Ruiz-Esparza et al., 2021; Sakai et al., 2015; Sultana et al., 2019, 2020; Yang et al., 2017; J. Yu et al., 2021; E. Zhang et al., 2017)

Ischemic conditions and a disrupted inflammatory response highlight the biological foundation of adhesions and thereby present an additional pathway to an augmented treatment approach. Localized anti-inflammatory release from an adherent fibrous polymer or hydrogel could inhibit the rapid fibroblast proliferation within a fibrin matrix presented in adhesions pathology. However, the process that contributes to adhesion formation cannot be completely prevented utilizing anti-inflammatory medications as it would also inhibit wound healing and immune response to infection. Hence, controlled release platforms are a necessity when designing a therapeutically focused adhesion barrier material. Jiang et al. introduces celecoxib — a non-steroidal anti-inflammatory drug (NSAID) — into a multi-layer, electrospun hyaluronic acid and poly(L-lactic acid)-polyethylene glycol structure as to inhibit fibroblast proliferation and collagen generation.(Jiang et al., 2015) Whether loaded drug directly elicits a reduction in fibrotic scar tissue deposition is unclear since rigorous in vitro release data is not provided, and there exists minimal basis for clinical assessment at 21 days in rabbit tendon anastomosis model. Li et al. instead studies utility of 10-hydroxycamptothecin and diclofenac sodium drugs in electrospun poly(ethylene glycol)-block-poly(L-lactide-co-glycolide) nanofibers.(J. Li et al., 2018) Minimal difference in percent release in tested formulations leads one to believe that a majority of drug diffuses out from polymer fibers in a burst fashion within the first few hours. Release of therapeutics in a controllable fashion is crucial in counteracting a 14-day fibrotic process, as cellular uptake rate and dose dependent toxicity are of great concern.(diZerega, 2001) Fibrous and hydrogel materials with drug release tuned exactly to fibrotic response following mesothelial tissue injury harness great potential as adhesion barriers.

Conclusion

Biomaterials developed in research laboratories frequently present reduced clinical translatability when applied in surgery, due to a combination of a non-optimized cohesion

and adhesion, extensive prefabrication methods, or prolonged application times to tissue substrates in vivo. Material selection plays a large role in respective metrics of efficacy such as wound area, adhesion strength, burst pressure, blood loss, and scar tissue severity. In wound dressing, hemostat, and adhesion barrier applications, one could contend cohesive strength is more favored, so the applied material does not fracture and still retains functionality. Whereas in tissue adhesive and surgical sealant applications, there is an argument for the greater importance of adhesiveness to tissue, so material is retained at the site of application. Furthermore, application methods further play a major role in dictating whether the material can be easily and rapidly applied in the fast-paced setting of an operating room. Such a wide variety of approaches to improving upon commercial materials is evidence that there is no singular solution for the variable clinical scenarios described.

Wound dressing materials seek to provide a sheath like protection for disrupted mesothelial tissue as to promote full tissue repair, and thus epidermal skin closure. Liang et al. presented exemplary data for their hybrid hyaluronic acid-dopamine hydrogel system with a two-fold (40% vs 80%) difference in skin contraction versus control in a full thickness, small mouse model (t = 7d).(Liang, Zhao, Hu, Han, et al., 2019) However, translation to more clinically relevant large animal models is diminished by subpar tissue adhesion strength on porcine skin (~5 kPa). Improved adhesive capabilities could lead to an even greater level of skin wound closure due to prolonged tissue retention and protection of damaged tissue. Often when one seeks to improve tissue adhesive capabilities though, the balance of cohesion and adhesion is compromised, and clinical effectiveness is reduced. This relation is particularly seen in a contrast with work by Han et al., where the team investigated a similar, dopamine-containing hydrogel that exhibited notably better level of adhesion on pig skin (~85 kPa), but reduced improvement in healing profile (50% vs 65%) in a full thickness rat model (t = 9d).(Han et al., 2016) Further exploration into sealant materials designed to withstand inflationary forces and seal defect sites exhibit similar behavior. Kelmansky et al. devised a PEG-NHS glue with extremely high adhesion to pig skin (~175 kPa) owing to the ability of the material to readily flow and facilitate nanoscale interactions with target tissue.(Kelmansky et al., 2017) While effective in topical applications requiring broad surface-to-surface adhesion, glue-based materials are extremely brittle upon drying and thus fail in metrics where cohesive capabilities are tested, such as burst pressure (~ 9 kPa) on a collagen membrane. When compared to results presented in Tables 5–6, the material studied by the authors is largely rendered ineffective with respect to sealant capabilities. Hemostatic materials exhibit a similarity to sealants in the sense that they too need withstand inflationary forces, but also exhibit an ability to rapidly plug blood flow without fracturing. Du et al. fabricated a chitosan-modified hydrogel that excelled in coagulation in a rat liver incision model, reducing blood loss from 375 mg to 20 mg and clotting time from 120 s to 30 s.(Du et al., 2020) However, tissue adhesion on pig skin (~ 8 kPa) and burst pressure on pig intestine (~ 10 kPa) greatly contrasts clinical potential for hemostatic applications of their material as compared to data in Tables 3–4 and Tables 5–6. Such comparisons highlight the fact that a simple linear or inverse correlation can’t be drawn, and that one material cannot be adopted ubiquitously for all discussed applications.

Prior to full clinical translation to patients, pilot studies in small scale animal models (mice, rats) followed by further studies in large scale animal models (piglet, sheep, non-human

primate) need be performed. Mice and rats are widely adopted in nanomaterials research for animal modeling due to biological and genetic similarities to humans, as well as lower costs when studied with large sample sizes.(Mortell et al., 2006) Small organisms are limited in their ability to replicate human physiology due to their gross anatomic and biomechanical differences, such as heartrate and respirations. (Ribitsch et al., 2020). It is for this reason that pig models have become a focus of researchers seeking to deploy materials in surgery, particularly in similarity with the human cardiovascular system, skin, and digestive tract. With extensive in vitro and in vivo data testing on relevant efficacy and safety (toxicity, biocompatibility, immunogenicity, etc.) metrics, approval by regulatory agencies such as the Food and Drug Administration (FDA) is the next step to bringing a material device to market and widescale adoption. Novel nanomaterials deployed in surgery require a premarket approval (PMA) and passage of a greater number of requirements due to their high-risk classification, while repurposing of existing materials requires a much less stringent FDA 510(k) premarket submission if deemed substantially equivalent. Deciding on which regulatory pathway to pursue in the early stages of an investigation is highly implicative in guiding research approach.

Despite countless rounds of data collection and review, approved materials present not only efficacy shortcomings for reasons aforementioned, but also a gross biocompatibility complication stemming from an inherent foreign body response (FBR). Implantation of a nanomaterial in vivo disrupts surrounding tissue and leads to a secretion of cytokines that drive recruitment of proteins, neutrophils, and macrophages in an attempt to degrade it. (Anderson et al., 2008; Carnicer-Lombarte et al., 2021) Non-degraded material is enveloped by fibrotic tissue as to physically isolate it from the rest of the body. When designing materials for surgical applications such as those above, it is important its degradability as well as alterations to local mechanical properties. Clinically approved wound dressings and tissue adhesives currently deployed in the clinic are often acrylate based in nature, and thus yield cytotoxic formaldehyde and unpolymerized acrylate byproducts as a result of hydrolytic degradation. (Pascual et al., 2016) Commercial sealant, hemostatic, and adhesion barrier materials are hydrogel-based materials that coupled with brittle nature upon swelling also enhance the FBR via augmented macrophage adhesion to material surface. (Swartzlander et al., 2015) Hence, it is crucial that independent research investigations understand the role of biodegradation and the FBR in nanomaterial design.

Future investigations into synthesizing polymeric materials for use in surgery could focus on scientific methods for creating rapid, non-toxic curing approaches in situ, as well as economic approaches to generating cost-effective treatment options. Biocompatible approaches highlighted in this review include 1) thermally mediated adhesion occurring at body temperature, 2) simple pressure application for use to applied substrate, and 3) use of non-toxic initiators for increasing adhesion at material-tissue interface whilst also fostering polymer network formation. Such methods would shift away from prevalent approaches of caustic initiators and ultraviolet light curing methods for generating nanolevel adhesion critical to enact relevant function. Coupled with further research innovations into devising surgical nanomaterials, it also important not to neglect economic impact and strategies for practical adoption. For example, dressing materials we have synthesized in the Kofinas and Sandler research groups for treatment of large porcine burn wounds cost ~$15 / wound.

(Carney et al., 2022) In spite of the clinical advantages of adhesiveness and biocompatibility, the need to optimize for cost is evident with the affordability of polyurethane-based films (Tegaderm, ~$1 / wound) and foams (Mepilex, ~$10 / wound). However, the simple synthesis of our solution blow spun fiber mats — via dissolution of polymer in solvent — provides a promising framework in pursuit of commercial scale-up. Further translation to clinical settings would also prove to be a small or nonexistent obstacle given the intuitive nature of spray deposition via an airbrush and availability of its pressure source (CO_2, compressed air) in operational conditions.

Funding Information

Research reported in this publication was supported by the National Institute of General Medical Sciences of the National Institutes of Health under Award Number R01GM141132. M.E. was supported by the National Institute of Diabetes and Digestive and Kidney Diseases of the National Institutes of Health under Award Number F31DK129021. The content is solely the responsibility of the authors and does not necessarily represent the official views of the National Institutes of Health.

References

Ahmed R, Tariq M, Ali I, Asghar R, Noorunnisa Khanam P, Augustine R, & Hasan A. (2018). Novel electrospun chitosan/polyvinyl alcohol/zinc oxide nanofibrous mats with antibacterial and antioxidant properties for diabetic wound healing. International Journal of Biological Macromolecules, 120, 385–393. 10.1016/j.ijbiomac.2018.08.057 [PubMed: 30110603]

Amiri N, Ajami S, Shahroodi A, Jannatabadi N, Amiri Darban S, Fazly Bazzaz BS, Pishavar E, Kalalinia F, & Movaffagh J. (2020). Teicoplanin-loaded chitosan-PEO nanofibers for local antibiotic delivery and wound healing. International Journal of Biological Macromolecules, 162, 645–656. 10.1016/j.ijbiomac.2020.06.195 [PubMed: 32585266]

Anderson JM, Rodriguez A, & Chang DT (2008). Foreign body reaction to biomaterials. Seminars in Immunology, 20(2), 86–100. 10.1016/j.smim.2007.11.004 [PubMed: 18162407]

Annabi N, Zhang Y-N, Assmann A, Sani ES, Cheng G, Lassaletta AD, Vegh A, Dehghani B, Ruiz-Esparza GU, Wang X, Gangadharan S, Weiss AS, & Khademhosseini A. (2017). Engineering a highly elastic human protein–based sealant for surgical applications. Science Translational Medicine, 9(410), eaai7466. 10.1126/scitranslmed.aai7466

Anthis AHC, Hu X, Matter MT, Neuer AL, Wei K, Schlegel AA, Starsich FHL, & Herrmann IK (2021). Chemically Stable, Strongly Adhesive Sealant Patch for Intestinal Anastomotic Leakage Prevention. Advanced Functional Materials, 31(16), 2007099. 10.1002/adfm.202007099

Assmann A, Vegh A, Ghasemi-Rad M, Bagherifard S, Cheng G, Sani ES, Ruiz-Esparza GU, Noshadi I, Lassaletta AD, Gangadharan S, Tamayol A, Khademhosseini A, & Annabi N. (2017). A highly adhesive and naturally derived sealant. Biomaterials, 140, 115–127. 10.1016/j.biomaterials.2017.06.004 [PubMed: 28646685]

Bai S, Zhang X, Cai P, Huang X, Huang Y, Liu R, Zhang M, Song J, Chen X, & Yang H. (2019). A silk-based sealant with tough adhesion for instant hemostasis of bleeding tissues. Nanoscale Horizons, 4(6), 1333–1341. 10.1039/C9NH00317G

Bang S, Lee E, Ko Y-G, Kim WI, & Kwon OH (2016). Injectable pullulan hydrogel for the prevention of postoperative tissue adhesion. International Journal of Biological Macromolecules, 87, 155–162. 10.1016/j.ijbiomac.2016.02.026 [PubMed: 26879910]

Behrens AM, Lee NG, Casey BJ, Srinivasan P, Sikorski MJ, Daristotle JL, Sandler AD, & Kofinas P. (2015). Biodegradable-Polymer-Blend-Based Surgical Sealant with Body-Temperature-Mediated Adhesion. Advanced Materials, 27(48), 8056–8061. 10.1002/adma.201503691 [PubMed: 26554545]

Behrens AM, Sikorski MJ, Li T, Wu ZJ, Griffith BP, & Kofinas P. (2014). Blood-aggregating hydrogel particles for use as a hemostatic agent. Acta Biomaterialia, 10(2), 701–708. 10.1016/j.actbio.2013.10.029 [PubMed: 24185001]

Blacklow SO, Li J, Freedman BR, Zeidi M, Chen C, & Mooney DJ (2019). Bioinspired mechanically active adhesive dressings to accelerate wound closure. Science Advances, 5(7), Article 7. 10.1126/sciadv.aaw3963

Bu Y, Zhang L, Sun G, Sun F, Liu J, Yang F, Tang P, & Wu D. (2019). Tetra-PEG Based Hydrogel Sealants for In Vivo Visceral Hemostasis. Advanced Materials, 31(28), 1901580. 10.1002/adma.201901580

Cai X, Hu S, Yu B, Cai Y, Yang J, Li F, Zheng Y, & Shi X. (2018). Transglutaminase-catalyzed preparation of crosslinked carboxymethyl chitosan/carboxymethyl cellulose/collagen composite membrane for postsurgical peritoneal adhesion prevention. Carbohydrate Polymers, 201, 201–210. 10.1016/j.carbpol.2018.08.065 [PubMed: 30241812]

Carney BC, Oliver MA, Erdi M, Kirkpatrick LD, Tranchina SP, Rozyyev S, Keyloun JW, Saruwatari MS, Daristotle JL, Moffatt LT, Kofinas P, Sandler AD, & Shupp JW (2022). Evaluation of healing outcomes combining a novel polymer formulation with autologous skin cell suspension to treat deep partial and full thickness wounds in a porcine model: A pilot study. Burns, 48(8), 1950–1965. 10.1016/j.burns.2022.01.012 [PubMed: 35151510]

Carnicer-Lombarte A, Chen S-T, Malliaras GG, & Barone DG (2021). Foreign Body Reaction to Implanted Biomaterials and Its Impact in Nerve Neuroprosthetics. Frontiers in Bioengineering and Biotechnology, 9. https://www.frontiersin.org/articles/10.3389/fbioe.2021.622524

Catena F, Ansaloni L, Di Saverio S, & Pinna AD (2012). P.O.P.A. Study: Prevention of Postoperative Abdominal Adhesions by Icodextrin 4% Solution After Laparotomy for Adhesive Small Bowel Obstruction. A Prospective Randomized Controlled Trial. Journal of Gastrointestinal Surgery, 16(2), 382–388. 10.1007/s11605-011-1736-y [PubMed: 22052104]

Chan LW, Wang X, Wei H, Pozzo LD, White NJ, & Pun SH (2015). A synthetic fibrin cross-linking polymer for modulating clot properties and inducing hemostasis. Science Translational Medicine, 7(277). 10.1126/scitranslmed.3010383

Chen C-H, Chen S-H, Mao S-H, Tsai M-J, Chou P-Y, Liao C-H, & Chen J-P (2017). Injectable thermosensitive hydrogel containing hyaluronic acid and chitosan as a barrier for prevention of postoperative peritoneal adhesion. Carbohydrate Polymers, 173, 721–731. 10.1016/j.carbpol.2017.06.019 [PubMed: 28732919]

Chen C-H, Chen S-H, Shalumon KT, & Chen J-P (2015). Prevention of peritendinous adhesions with electrospun polyethylene glycol/polycaprolactone nanofibrous membranes. Colloids and Surfaces B: Biointerfaces, 133, 221–230. 10.1016/j.colsurfb.2015.06.012 [PubMed: 26115533]

Chen G, Yu Y, Wu X, Wang G, Ren J, & Zhao Y. (2018). Bioinspired Multifunctional Hybrid Hydrogel Promotes Wound Healing. Advanced Functional Materials, 28(33), 1801386. 10.1002/adfm.201801386

Chen S, Carlson MA, Zhang YS, Hu Y, & Xie J. (2018). Fabrication of injectable and superelastic nanofiber rectangle matrices (“peanuts”) and their potential applications in hemostasis. Biomaterials, 179, 46–59. 10.1016/j.biomaterials.2018.06.031 [PubMed: 29980074]

Chen T, Chen Y, Rehman HU, Chen Z, Yang Z, Wang M, Li H, & Liu H. (2018). Ultratough, Self-Healing, and Tissue-Adhesive Hydrogel for Wound Dressing. ACS Applied Materials & Interfaces, 10(39), 33523–33531. 10.1021/acsami.8b10064 [PubMed: 30204399]

Chen W, Wang R, Xu T, Ma X, Yao Z, Chi B, & Xu H. (2017). A mussel-inspired poly(γ-glutamic acid) tissue adhesive with high wet strength for wound closure. J. Mater. Chem. B, 5(28), Article 28. 10.1039/C7TB00813A

Church D, Elsayed S, Reid O, Winston B, & Lindsay R. (2006). Burn Wound Infections. CLIN. MICROBIOL. REV, 19, 32.

Daristotle JL, Behrens AM, Sandler AD, & Kofinas P. (2016). A Review of the Fundamental Principles and Applications of Solution Blow Spinning. ACS Applied Materials & Interfaces, 8(51), 34951–34963. 10.1021/acsami.6b12994 [PubMed: 27966857]

Daristotle JL, Erdi M, Lau LW, Zaki ST, Srinivasan P, Balabhadrapatruni M, Ayyub OB, Sandler AD, & Kofinas P. (2021). Biodegradable, Tissue Adhesive Polyester Blends for Safe, Complete Wound Healing. ACS Biomaterials Science & Engineering, 7(8), 3908–3916. 10.1021/acsbiomaterials.1c00865 [PubMed: 34323468]

Daristotle JL, Lau LW, Erdi M, Hunter J, Djoum A, Srinivasan P, Wu X, Basu M, Ayyub OB, Sandler AD, & Kofinas P. (2020). Sprayable and Biodegradable, Intrinsically Adhesive Wound Dressing with Antimicrobial Properties. Bioengineering & Translational Medicine, 5(1). 10.1002/btm2.10149

Daristotle JL, Zaki ST, Lau LW, Ayyub OB, Djouini M, Srinivasan P, Erdi M, Sandler AD, & Kofinas P. (2020). Pressure-Sensitive Tissue Adhesion and Biodegradation of Viscoelastic Polymer Blends. ACS Applied Materials & Interfaces, 12(14), 16050–16057. 10.1021/acsami.0c00497 [PubMed: 32191429]

Daristotle JL, Zaki ST, Lau LW, Torres L, Zografos A, Srinivasan P, Ayyub OB, Sandler AD, & Kofinas P. (2019). Improving the Adhesion, Flexibility, and Hemostatic Efficacy of a Sprayable Polymer Blend Surgical Sealant by Incorporating Silica Particles. Acta Biomaterialia, 90, 205–216. 10.1016/j.actbio.2019.04.015 [PubMed: 30954624]

Deng X. (2018). Progress on rubber-based pressure-sensitive adhesives. The Journal of Adhesion, 94(2), 77–96. 10.1080/00218464.2016.1249573

Deuling J. h. h., Vermeulen R. p., Anthonio R. a., van den Heuvel A. f. m., Jaarsma T, Jessurun G, de Smet B. j. g. l., Tan E. s., & Zijlstra F. (2008). Closure of the femoral artery after cardiac catheterization: A comparison of Angio-Seal, StarClose, and manual compression. Catheterization and Cardiovascular Interventions, 71(4), 518–523. 10.1002/ccd.21429 [PubMed: 18307223]

diZerega GS (2001). Peritoneal Repair and Post-Surgical Adhesion Formation. Human Reproduction Update, 7(6), 547–555. 10.1093/humupd/7.6.547 [PubMed: 11727863]

Dowling MB, Smith W, Balogh P, Duggan MJ, MacIntire IC, Harris E, Mesar T, Raghavan SR, & King DR (2015). Hydrophobically-modified chitosan foam: Description and hemostatic efficacy. Journal of Surgical Research, 193(1), 316–323. 10.1016/j.jss.2014.06.019 [PubMed: 25016441]

Du X, Liu Y, Yan H, Rafique M, Li S, Shan X, Wu L, Qiao M, Kong D, & Wang L. (2020). Anti-Infective and Pro-Coagulant Chitosan-Based Hydrogel Tissue Adhesive for Sutureless Wound Closure. Biomacromolecules, 21(3), Article 3. 10.1021/acs.biomac.9b01707

Dunn LL, de Valence S, Tille J-C, Hammel P, Walpoth BH, Stocker R, Imhof BA, & Miljkovic-Licina M. (2016). Biodegradable and plasma-treated electrospun scaffolds coated with recombinant Olfactomedin-like 3 for accelerating wound healing and tissue regeneration: Matricellular protein olfactomedin-like 3 promotes neovascularization. Wound Repair and Regeneration, 24(6), Article 6. 10.1111/wrr.12485

Erdi M, Rozyyev S, Balabhadrapatruni M, Saruwatari MS, Daristotle JL, Ayyub OB, Sandler AD, & Kofinas P. (2022). Sprayable Tissue Adhesive with Biodegradation Tuned for Prevention of Postoperative Abdominal Adhesions. Bioengineering & Translational Medicine, e10335. 10.1002/btm2.10335

Evans JA, van Wessem KJP, McDougall D, Lee KA, Lyons T, & Balogh ZJ (2010). Epidemiology of Traumatic Deaths: Comprehensive Population-Based Assessment. World Journal of Surgery, 34(1), 158–163. 10.1007/s00268-009-0266-1 [PubMed: 19882185]

Falsafi A, Tirrell M, & Pocius AV (2000). Compositional Effects on the Adhesion of Acrylic Pressure Sensitive Adhesives. Langmuir, 16(4), Article 4. 10.1021/la990345z

Fan C, Fu J, Zhu W, & Wang D-A (2016). A mussel-inspired double-crosslinked tissue adhesive intended for internal medical use. Acta Biomaterialia, 33, 51–63. 10.1016/j.actbio.2016.02.003 [PubMed: 26850148]

Fathi P, Sikorski M, Christodoulides K, Langan K, Choi YS, Titcomb M, Ghodasara A, Wonodi O, Thaker H, Vural M, Behrens A, & Kofinas P. (2018). Zeolite-loaded alginate-chitosan hydrogel beads as a topical hemostat: Zeolite-loaded alginate-chitosan hydrogel. Journal of Biomedical Materials Research Part B: Applied Biomaterials, 106(5), 1662–1671. 10.1002/jbm.b.33969 [PubMed: 28842967]

Felton L. (1997). Influence of plasticizers on the adhesive properties of an acrylic resin copolymer to hydrophilic and hydrophobic tablet compacts. International Journal of Pharmaceutics, 154(2), 167–178. 10.1016/S0378-5173(97)00133-6

Fernandez JG, Seetharam S, Ding C, Feliz J, Doherty E, & Ingber DE (2017). Direct Bonding of Chitosan Biomaterials to Tissues Using Transglutaminase for Surgical Repair or Device Implantation. Tissue Engineering Part A, 23(3–4), 135–142. 10.1089/ten.tea.2016.0266 [PubMed: 27869543]

Field CK, & Kerstein MD (1994). Overview of wound healing in a moist environment. The American Journal of Surgery, 167(1), S2–S6. 10.1016/0002-9610(94)90002-7

Fuller C. (2013). Reduction of intraoperative air leaks with Progel in pulmonary resection: A comprehensive review. Journal of Cardiothoracic Surgery, 8(1), 90. 10.1186/1749-8090-8-90 [PubMed: 23590942]

Gan D, Xu T, Xing W, Ge X, Fang L, Wang K, Ren F, & Lu X. (2019). Mussel-Inspired Contact-Active Antibacterial Hydrogel with High Cell Affinity, Toughness, and Recoverability. Advanced Functional Materials, 29(1), 1805964. 10.1002/adfm.201805964

GhavamiNejad A, Park CH, & Kim CS (2016). In Situ Synthesis of Antimicrobial Silver Nanoparticles within Antifouling Zwitterionic Hydrogels by Catecholic Redox Chemistry for Wound Healing Application. Biomacromolecules, 17(3), 1213–1223. 10.1021/acs.biomac.6b00039 [PubMed: 26891456]

Greiner A, & Wendorff JH (2007). Electrospinning: A Fascinating Method for the Preparation of Ultrathin Fibers. Angewandte Chemie International Edition, 46(30), 5670–5703. 10.1002/anie.200604646 [PubMed: 17585397]

Griffin DR, Weaver WM, Scumpia PO, Di Carlo D, & Segura T. (2015). Accelerated wound healing by injectable microporous gel scaffolds assembled from annealed building blocks. Nature Materials, 14(7), 737–744. 10.1038/nmat4294 [PubMed: 26030305]

Guo S, Yao M, Zhang D, He Y, Chang R, Ren Y, & Guan F. (2022). One-Step Synthesis of Multifunctional Chitosan Hydrogel for Full-Thickness Wound Closure and Healing. Advanced Healthcare Materials, 11(4), 2101808. 10.1002/adhm.202101808

Han L, Lu X, Liu K, Wang K, Fang L, Weng L-T, Zhang H, Tang Y, Ren F, Zhao C, Sun G, Liang R, & Li Z. (2017). Mussel-Inspired Adhesive and Tough Hydrogel Based on Nanoclay Confined Dopamine Polymerization. ACS Nano, 11(3), 2561–2574. 10.1021/acsnano.6b05318 [PubMed: 28245107]

Han L, Wang M, Li P, Gan D, Yan L, Xu J, Wang K, Fang L, Chan CW, Zhang H, Yuan H, & Lu X. (2018). Mussel-Inspired Tissue-Adhesive Hydrogel Based on the Polydopamine–Chondroitin Sulfate Complex for Growth-Factor-Free Cartilage Regeneration. ACS Applied Materials & Interfaces, 10(33), 28015–28026. 10.1021/acsami.8b05314 [PubMed: 30052419]

Han L, Yan L, Wang K, Fang L, Zhang H, Tang Y, Ding Y, Weng L, Xu J, Weng J, Liu Y, Ren F, & Lu X. (2017). Tough, self-healable and tissue-adhesive hydrogel with tunable multifunctionality. NPG Asia Materials, 9(4), n/a. 10.1038/am.2017.33

Han L, Zhang Y, Lu X, Wang K, Wang Z, & Zhang H. (2016). Polydopamine Nanoparticles Modulating Stimuli-Responsive PNIPAM Hydrogels with Cell/Tissue Adhesiveness. ACS Applied Materials & Interfaces, 8(42), Article 42. 10.1021/acsami.6b11043

Hanthamrongwit M, Reid WH, & Grant MH (1996). Chondroitin-6-sulphate incorporated into collagen gels for the growth of human keratinocytes: The effect of cross-linking agents and diamines. Biomaterials, 17(8), 775–780. 10.1016/0142-9612(96)81414-1 [PubMed: 8730961]

He J, Shi M, Liang Y, & Guo B. (2020). Conductive adhesive self-healing nanocomposite hydrogel wound dressing for photothermal therapy of infected full-thickness skin wounds. Chemical Engineering Journal, 394, 124888. 10.1016/j.cej.2020.124888

He M, Sun L, Fu X, McDonough SP, & Chu C-C (2019). Biodegradable amino acid-based poly(ester amine) with tunable immunomodulating properties and their in vitro and in vivo wound healing studies in diabetic rats' wounds. Acta Biomaterialia, 84, 114–132. 10.1016/j.actbio.2018.11.053 [PubMed: 30508656]

He X, Liu L, Han H, Shi W, Yang W, & Lu X. (2019). Bioinspired and Microgel-Tackified Adhesive Hydrogel with Rapid Self-Healing and High Stretchability. Macromolecules, 52(1), Article 1. 10.1021/acs.macromol.8b01678

Hermanson GT (2013). Bioconjugate techniques (Third edition). Elsevier/AP.

Hong Y, Zhou F, Hua Y, Zhang X, Ni C, Pan D, Zhang Y, Jiang D, Yang L, Lin Q, Zou Y, Yu D, Arnot DE, Zou X, Zhu L, Zhang S, & Ouyang H. (2019). A strongly adhesive hemostatic hydrogel for the repair of arterial and heart bleeds. Nature Communications, 10(1), 2060. 10.1038/s41467-019-10004-7

Hoque J, Prakash RG, Paramanandham K, Shome BR, & Haldar J. (2017). Biocompatible Injectable Hydrogel with Potent Wound Healing and Antibacterial Properties. Molecular Pharmaceutics, 14(4), 1218–1230. 10.1021/acs.molpharmaceut.6b01104 [PubMed: 28207269]

Hsu BB, Conway W, Tschabrunn CM, Mehta M, Perez-Cuevas MB, Zhang S, & Hammond PT (2015). Clotting Mimicry from Robust Hemostatic Bandages Based on Self-Assembling Peptides. ACS Nano, 9(9), 9394–9406. 10.1021/acsnano.5b02374 [PubMed: 26284753]

Huang W, Wang Y, Huang Z, Wang X, Chen L, Zhang Y, & Zhang L. (2018). On-Demand Dissolvable Self-Healing Hydrogel Based on Carboxymethyl Chitosan and Cellulose Nanocrystal for Deep Partial Thickness Burn Wound Healing. ACS Applied Materials & Interfaces, 10(48), 41076–41088. 10.1021/acsami.8b14526 [PubMed: 30398062]

Huang Y, Zhao X, Zhang Z, Liang Y, Yin Z, Chen B, Bai L, Han Y, & Guo B. (2020). Degradable Gelatin-Based IPN Cryogel Hemostat for Rapidly Stopping Deep Noncompressible Hemorrhage and Simultaneously Improving Wound Healing. Chemistry of Materials, 32(15), 6595–6610. 10.1021/acs.chemmater.0c02030

Jeon EY, Lee J, Kim BJ, Joo KI, Kim KH, Lim G, & Cha HJ (2019). Bio-inspired swellable hydrogel-forming double-layered adhesive microneedle protein patch for regenerative internal/external surgical closure. Biomaterials, 222, 119439. 10.1016/j.biomaterials.2019.119439

Jiang S, Yan H, Fan D, Song J, & Fan C. (2015). Multi-Layer Electrospun Membrane Mimicking Tendon Sheath for Prevention of Tendon Adhesions. International Journal of Molecular Sciences, 16(12), 6932–6944. 10.3390/ijms16046932 [PubMed: 25822877]

Ju HW, Lee OJ, Lee JM, Moon BM, Park HJ, Park YR, Lee MC, Kim SH, Chao JR, Ki CS, & Park CH (2016). Wound healing effect of electrospun silk fibroin nanomatrix in burn-model. International Journal of Biological Macromolecules, 85, 29–39. 10.1016/j.ijbiomac.2015.12.055 [PubMed: 26718866]

Junker JP, Kamel RA, Caterson EJ, & Eriksson E. (2013). Clinical Impact Upon Wound Healing and Inflammation in Moist, Wet, and Dry Environments. Adv Wound Care (New Rochelle), 2(7), Article 7. 10.1089/wound.2012.0412

Kelly JF, Ritenour AE, McLaughlin DF, Bagg KA, Apodaca AN, Mallak CT, Pearse L, Lawnick MM, Champion HR, Wade CE, & Holcomb JB (2008). Injury Severity and Causes of Death From Operation Iraqi Freedom and Operation Enduring Freedom: 2003–2004 Versus 2006. Journal of Trauma: Injury, Infection & Critical Care, 64(2), S21–S27. 10.1097/TA.0b013e318160b9fb

Kelmansky R, McAlvin BJ, Nyska A, Dohlman JC, Chiang HH, Hashimoto M, Kohane DS, & Mizrahi B. (2017). Strong tissue glue with tunable elasticity. Acta Biomaterialia, 53, 93–99. 10.1016/j.actbio.2017.02.009 [PubMed: 28189813]

Kern NG, Behrens AM, Srinivasan P, Rossi CT, Daristotle JL, Kofinas P, & Sandler AD (2017). Solution Blow Spun Polymer: A Novel Preclinical Surgical Sealant for Bowel Anastomoses. Journal of Pediatric Surgery, 52(8), 1308–1312. 10.1016/j.jpedsurg.2016.11.044 [PubMed: 27956071]

Kim HJ, Hwang BH, Lim S, Choi B-H, Kang SH, & Cha HJ (2015). Mussel adhesion-employed water-immiscible fluid bioadhesive for urinary fistula sealing. Biomaterials, 72, 104–111. 10.1016/j.biomaterials.2015.08.055 [PubMed: 26352517]

Kim YS (1974). Human Tissues: Chemical Composition and Photon Dosimetry Data. Radiation Research, 57(1), 38. 10.2307/3573753 [PubMed: 10874926]

Kinloch AJ (1980). The science of adhesion. Journal of Materials Science, 15(9), 2141–2166. 10.1007/BF00552302

Kord Forooshani P, & Lee BP (2017). Recent approaches in designing bioadhesive materials inspired by mussel adhesive protein. Journal of Polymer Science Part A: Polymer Chemistry, 55(1), 9–33. 10.1002/pola.28368 [PubMed: 27917020]

Lan G, Lu B, Wang T, Wang L, Chen J, Yu K, Liu J, Dai F, & Wu D. (2015). Chitosan/gelatin composite sponge is an absorbable surgical hemostatic agent. Colloids and Surfaces B: Biointerfaces, 136, 1026–1034. 10.1016/j.colsurfb.2015.10.039 [PubMed: 26590895]

Lang N, Pereira MJ, Lee Y, Friehs I, Vasilyev NV, Feins EN, Ablasser K, O'Cearbhaill ED, Xu C, Fabozzo A, Padera R, Wasserman S, Freudenthal F, Ferreira LS, Langer R, Karp JM, & del Nido

PJ (2014). A Blood-Resistant Surgical Glue for Minimally Invasive Repair of Vessels and Heart Defects. Science Translational Medicine, 6(218). 10.1126/scitranslmed.3006557

Leberfinger A, Hospodiuk M, Pena-Francesch A, Ayan B, Ozbolat V, Koduru S, Ozbolat I, Demirel MC, & Ravnic D. (2018). Squid Ring Teeth-coated Mesh Improves Abdominal Wall Repair. Plast Reconstr Surg Glob Open, 6, e1881. 10.1101/214114 [PubMed: 30254828]

Lee JN, Lee SY, & Park WH (2021). Bioinspired Self-Healable Polyallylamine-Based Hydrogels for Wet Adhesion: Synergistic Contributions of Catechol-Amino Functionalities and Nanosilicate. ACS Applied Materials & Interfaces, 13(15), 18324–18337. 10.1021/acsami.1c02141 [PubMed: 33840193]

Lee Y, Xu C, Sebastin M, Lee A, Holwell N, Xu C, Miranda Nieves D, Mu L, Langer RS, Lin C, & Karp JM (2015). Bioinspired Nanoparticulate Medical Glues for Minimally Invasive Tissue Repair. Advanced Healthcare Materials, 4(16), 2587–2596. 10.1002/adhm.201500419 [PubMed: 26227833]

Li J, Xu W, Chen J, Li D, Zhang K, Liu T, Ding J, & Chen X. (2018). Highly Bioadhesive Polymer Membrane Continuously Releases Cytostatic and Anti-Inflammatory Drugs for Peritoneal Adhesion Prevention. ACS Biomaterials Science & Engineering, 4(6), 2026–2036. 10.1021/acsbiomaterials.7b00605 [PubMed: 33445273]

Li M, Zhang Z, Liang Y, He J, & Guo B. (2020). Multifunctional Tissue-Adhesive Cryogel Wound Dressing for Rapid Nonpressing Surface Hemorrhage and Wound Repair. ACS Applied Materials & Interfaces, 12(32), 35856–35872. 10.1021/acsami.0c08285 [PubMed: 32805786]

Li S, Zhou J, Huang Y, Roy J, Zhou N, Yum K, Sun X, & Tang L. (2020). Injectable Click Chemistry-based Bioadhesives for Accelerated Wound Closure. Acta Biomaterialia, 110, 95–104. 10.1016/j.actbio.2020.04.004 [PubMed: 32362581]

Li Z, Liu L, & Chen Y. (2020). Dual dynamically crosslinked thermosensitive hydrogel with self-fixing as a postoperative anti-adhesion barrier. Acta Biomaterialia, 110, 119–128. 10.1016/j.actbio.2020.04.034 [PubMed: 32438111]

Liang Y, Chen B, Li M, He J, Yin Z, & Guo B. (2020). Injectable Antimicrobial Conductive Hydrogels for Wound Disinfection and Infectious Wound Healing. Biomacromolecules, 21(5), 1841–1852. 10.1021/acs.biomac.9b01732 [PubMed: 32388998]

Liang Y, Zhao X, Hu T, Chen B, Yin Z, Ma PX, & Guo B. (2019). Adhesive Hemostatic Conducting Injectable Composite Hydrogels with Sustained Drug Release and Photothermal Antibacterial Activity to Promote Full-Thickness Skin Regeneration During Wound Healing. Small, 15(12), 1900046. 10.1002/smll.201900046

Liang Y, Zhao X, Hu T, Han Y, & Guo B. (2019). Mussel-inspired, antibacterial, conductive, antioxidant, injectable composite hydrogel wound dressing to promote the regeneration of infected skin. Journal of Colloid and Interface Science, 556, 514–528. 10.1016/j.jcis.2019.08.083 [PubMed: 31473541]

Liu C, Liu X, Liu C, Wang N, Chen H, Yao W, Sun G, Song Q, & Qiao W. (2019). A highly efficient, in situ wet-adhesive dextran derivative sponge for rapid hemostasis. Biomaterials, 205, 23–37. 10.1016/j.biomaterials.2019.03.016 [PubMed: 30901635]

Liu C, Yao W, Tian M, Wei J, Song Q, & Qiao W. (2018). Mussel-inspired degradable antibacterial polydopamine/silica nanoparticle for rapid hemostasis. Biomaterials, 179, 83–95. 10.1016/j.biomaterials.2018.06.037 [PubMed: 29980077]

Liu Y, Meng H, Konst S, Sarmiento R, Rajachar R, & Lee BP (2014). Injectable Dopamine-Modified Poly(ethylene glycol) Nanocomposite Hydrogel with Enhanced Adhesive Property and Bioactivity. ACS Applied Materials & Interfaces, 6(19), 16982–16992. 10.1021/am504566v [PubMed: 25222290]

Lokhande G, Carrow JK, Thakur T, Xavier JR, Parani M, Bayless KJ, & Gaharwar AK (2018). Nanoengineered injectable hydrogels for wound healing application. Acta Biomaterialia, 70, 35–47. 10.1016/j.actbio.2018.01.045 [PubMed: 29425720]

Lu Z, Gao J, He Q, Wu J, Liang D, Yang H, & Chen R. (2017). Enhanced antibacterial and wound healing activities of microporous chitosan-Ag/ZnO composite dressing. Carbohydrate Polymers, 156, 460–469. 10.1016/j.carbpol.2016.09.051 [PubMed: 27842847]

Luo J-W, Liu C, Wu J-H, Lin L-X, Fan H-M, Zhao D-H, Zhuang Y-Q, & Sun Y-L (2019). In situ injectable hyaluronic acid/gelatin hydrogel for hemorrhage control. Materials Science and Engineering: C, 98, 628–634. 10.1016/j.msec.2019.01.034

Ma R, Wang Y, Qi H, Shi C, Wei G, Xiao L, Huang Z, Liu S, Yu H, Teng C, Liu H, Murugadoss V, Zhang J, Wang Y, & Guo Z. (2019). Nanocomposite sponges of sodium alginate/graphene oxide/polyvinyl alcohol as potential wound dressing: In vitro and in vivo evaluation. Composites Part B: Engineering, 167, 396–405. 10.1016/j.compositesb.2019.03.006

Mao Y, Li P, Yin J, Bai Y, Zhou H, Lin X, Yang H, & Yang L. (2021). Starch-based adhesive hydrogel with gel-point viscoelastic behavior and its application in wound sealing and hemostasis. Journal of Materials Science & Technology, 63, 228–235. 10.1016/j.jmst.2020.02.071

Mayes SM, Davis J, Scott J, Aguilar V, Zawko SA, Swinnea S, Peterson DL, Hardy JG, & Schmidt CE (2020). Polysaccharide-based films for the prevention of unwanted postoperative adhesions at biological interfaces. Acta Biomaterialia, 106, 92–101. 10.1016/j.actbio.2020.02.027 [PubMed: 32097711]

Medeiros ES, Glenn GM, Klamczynski AP, Orts WJ, & Mattoso LHC (2009). Solution blow spinning: A new method to produce micro- and nanofibers from polymer solutions. Journal of Applied Polymer Science, 113(4), 2322–2330. 10.1002/app.30275

Menzies D. (1992). Peritoneal adhesions. Incidence, cause, and prevention. Surgery Annual, 24 Pt 1, 27–45. [PubMed: 1727325]

Menzies D. (1993). Postoperative adhesions: Their treatment and relevance in clinical practice. Annals of the Royal College of Surgeons of England, 75(3), 147–153. PubMed.

Menzies D, & Ellis H. (1990). Intestinal obstruction from adhesions—How big is the problem? Annals of The Royal College of Surgeons of England, 72(1), 60–63. [PubMed: 2301905]

Mortell A, Montedonico S, & Puri P. (2006). Animal models in pediatric surgery. Pediatric Surgery International, 22(2), 111–128. 10.1007/s00383-005-1593-4 [PubMed: 16331525]

Moscowitz I, & Wexner SD (2000). Contributions of Adhesions to the Cost of Healthcare. In diZerega GS (Ed.), Peritoneal Surgery (pp. 335–342). Springer New York. 10.1007/978-1-4612-1194-5_30

Nam S, & Mooney D. (2021). Polymeric Tissue Adhesives. Chemical Reviews, 121(18), 11336–11384. 10.1021/acs.chemrev.0c00798 [PubMed: 33507740]

Nishiguchi A, & Taguchi T. (2020). Designing an anti-inflammatory and tissue-adhesive colloidal dressing for wound treatment. Colloids and Surfaces B: Biointerfaces, 110737. 10.1016/j.colsurfb.2019.110737

Okada M, Nakai A, Hara ES, Taguchi T, Nakano T, & Matsumoto T. (2017). Biocompatible nanostructured solid adhesives for biological soft tissues. Acta Biomaterialia, 57, 404–413. 10.1016/j.actbio.2017.05.014 [PubMed: 28483692]

Ostomel TA, Shi Q, Stoimenov PK, & Stucky GD (2007). Metal Oxide Surface Charge Mediated Hemostasis. Langmuir, 23(22), Article 22. 10.1021/la701281t

Pascual G, Sotomayor S, Rodríguez M, Pérez-Köhler B, Kühnhardt A, Fernández-Gutiérrez M, San Román J, & Bellón JM (2016). Cytotoxicity of Cyanoacrylate-Based Tissue Adhesives and Short-Term Preclinical In Vivo Biocompatibility in Abdominal Hernia Repair. PLOS ONE, 11(6), e0157920. 10.1371/journal.pone.0157920

Peppas NA, & Buri PA (1985). Surface, interfacial and molecular aspects of polymer bioadhesion on soft tissues. Journal of Controlled Release, 2, 257–275. 10.1016/0168-3659(85)90050-1

Pinnaratip R, Meng H, Rajachar RM, & Lee BP (2018). Effect of incorporating clustered silica nanoparticles on the performance and biocompatibility of catechol-containing PEG-based bioadhesive. Biomedical Materials, 13(2), 025003. 10.1088/1748-605X/aa985d

Polat Y, Pampal ES, Stojanovska E, Simsek R, Hassanin A, Kilic A, Demir A, & Yilmaz S. (2016). Solution blowing of thermoplastic polyurethane nanofibers: A facile method to produce flexible porous materials. Journal of Applied Polymer Science, 133(9). 10.1002/app.43025

Powell HM, & Boyce ST (2006). EDC cross-linking improves skin substitute strength and stability. Biomaterials, 27(34), 5821–5827. 10.1016/j.biomaterials.2006.07.030 [PubMed: 16919327]

Qu J, Zhao X, Liang Y, Zhang T, Ma PX, & Guo B. (2018). Antibacterial adhesive injectable hydrogels with rapid self-healing, extensibility and compressibility as wound dressing for joints

skin wound healing. Biomaterials, 183, 185–199. 10.1016/j.biomaterials.2018.08.044 [PubMed: 30172244]

Ribitsch I, Baptista PM, Lange-Consiglio A, Melotti L, Patruno M, Jenner F, Schnabl-Feichter E, Dutton LC, Connolly DJ, van Steenbeek FG, Dudhia J, & Penning LC (2020). Large Animal Models in Regenerative Medicine and Tissue Engineering: To Do or Not to Do. Frontiers in Bioengineering and Biotechnology, 8, 972. 10.3389/fbioe.2020.00972 [PubMed: 32903631]

Ruiz-Esparza GU, Wang X, Zhang X, Jimenez-Vazquez S, Diaz-Gomez L, Lavoie A-M, Afewerki S, Fuentes-Baldemar AA, Parra-Saldivar R, Jiang N, Annabi N, Saleh B, Yetisen AK, Sheikhi A, Jozefiak TH, Shin SR, Dong N, & Khademhosseini A. (2021). Nanoengineered Shear-Thinning Hydrogel Barrier for Preventing Postoperative Abdominal Adhesions. Nano-Micro Letters, 13(1), 212. 10.1007/s40820-021-00712-5 [PubMed: 34664123]

Ryu JH, Kim HJ, Kim K, Yoon G, Wang Y, Choi G, Lee H, & Park JS (2019). Multipurpose Intraperitoneal Adhesive Patches. Advanced Functional Materials, 29(29), 1900495. 10.1002/adfm.201900495

Ryu JH, Messersmith PB, & Lee H. (2018). Polydopamine Surface Chemistry: A Decade of Discovery. ACS Applied Materials & Interfaces, 10(9), 7523–7540. 10.1021/acsami.7b19865 [PubMed: 29465221]

Sakai S, Ueda K, & Taya M. (2015). Peritoneal adhesion prevention by a biodegradable hyaluronic acid-based hydrogel formed in situ through a cascade enzyme reaction initiated by contact with body fluid on tissue surfaces. Acta Biomaterialia, 24, 152–158. 10.1016/j.actbio.2015.06.023 [PubMed: 26102338]

Shimony N, Shagan A, Eylon B, Nyska A, Gross A, & Mizrahi B. (2021). Liquid Copolymers as Biodegradable Surgical Sealant. Advanced Healthcare Materials, 10(19), 2100803. 10.1002/adhm.202100803

Shin J, Martello MT, Shrestha M, Wissinger JE, Tolman WB, & Hillmyer MA (2011). Pressure-Sensitive Adhesives from Renewable Triblock Copolymers. Macromolecules, 44(1), 87–94. 10.1021/ma102216d

Shirzaei Sani E, Kheirkhah A, Rana D, Sun Z, Foulsham W, Sheikhi A, Khademhosseini A, Dana R, & Annabi N. (2019). Sutureless repair of corneal injuries using naturally derived bioadhesive hydrogels. Science Advances, 5(3), Article 3. 10.1126/sciadv.aav1281

Shirzaei Sani E, Portillo Lara R, Aldawood Z, Bassir SH, Nguyen D, Kantarci A, Intini G, & Annabi N. (2019). An Antimicrobial Dental Light Curable Bioadhesive Hydrogel for Treatment of Peri-Implant Diseases. Matter, 1(4), Article 4. 10.1016/j.matt.2019.07.019

Singer AJ, Perry LC, & Allen RL Jr (2008). In Vivo Study of Wound Bursting Strength and Compliance of Topical Skin Adhesives. Academic Emergency Medicine, 15(12), 1290–1294. 10.1111/j.1553-2712.2008.00273.x [PubMed: 18945227]

Singer AJ, Quinn JV, & Hollander JE (2008). The cyanoacrylate topical skin adhesives. The American Journal of Emergency Medicine, 26(4), Article 4. 10.1016/j.ajem.2007.05.015

Singh A, Halder S, Chumber S, Misra MC, Sharma LK, Srivastava A, & Menon GR (2004). Meta-analysis of Randomized Controlled Trials on Hydrocolloid Occlusive Dressing Versus Conventional Gauze Dressing in the Healing of Chronic Wounds. Asian Journal of Surgery, 27(4), 326–332. 10.1016/S1015-9584(09)60061-0 [PubMed: 15564189]

Song L, Li L, He T, Wang N, Yang S, Yang X, Zeng Y, Zhang W, Yang L, Wu Q, & Gong C. (2016). Peritoneal adhesion prevention with a biodegradable and injectable N,O-carboxymethyl chitosan-aldehyde hyaluronic acid hydrogel in a rat repeated-injury model. Scientific Reports, 6(1), Article 1. 10.1038/srep37600

Spotnitz WD (2010). Fibrin Sealant: Past, Present, and Future: A Brief Review. World Journal of Surgery, 34(4), 632–634. 10.1007/s00268-009-0252-7 [PubMed: 19820991]

Spotnitz WD, & Burks S. (2012). Hemostats, sealants, and adhesives III: A new update as well as cost and regulatory considerations for components of the surgical toolbox. Transfusion, 52(10), Article 10. 10.1111/j.1537-2995.2012.03707.x

Stapleton LM, Lucian HJ, Grosskopf AK, Smith AAA, Totherow KP, Woo YJ, & Appel EA (2021). Dynamic Hydrogels for Prevention of Post-Operative Peritoneal Adhesions. Advanced Therapeutics, 4(3), 2000242. 10.1002/adtp.202000242

Stapleton LM, Steele AN, Wang H, Lopez Hernandez H, Yu AC, Paulsen MJ, Smith AAA, Roth GA, Thakore AD, Lucian HJ, Totherow KP, Baker SW, Tada Y, Farry JM, Eskandari A, Hironaka CE, Jaatinen KJ, Williams KM, Bergamasco H, … Woo YJ (2019). Use of a supramolecular polymeric hydrogel as an effective post-operative pericardial adhesion barrier. Nature Biomedical Engineering, 3(8), Article 8. 10.1038/s41551-019-0442-z

Sultana T, Gwon J-G, & Lee B-T (2020). Thermal stimuli-responsive hyaluronic acid loaded cellulose based physical hydrogel for post-surgical de novo peritoneal adhesion prevention. Materials Science and Engineering: C, 110661. 10.1016/j.msec.2020.110661

Sultana T, Van Hai H, Abueva C, Kang HJ, Lee S-Y, & Lee B-T (2019). TEMPO oxidized nano-cellulose containing thermo-responsive injectable hydrogel for post-surgical peritoneal tissue adhesion prevention. Materials Science and Engineering: C, 102, 12–21. 10.1016/j.msec.2019.03.110

Sun F, Bu Y, Chen Y, Yang F, Yu J, & Wu D. (2020). An Injectable and Instant Self-Healing Medical Adhesive for Wound Sealing. ACS Applied Materials & Interfaces, 12(8), 9132–9140. 10.1021/acsami.0c01022 [PubMed: 32058692]

Suneetha M, Rao KM, & Han SS (2019). Mussel-Inspired Cell/Tissue-Adhesive, Hemostatic Hydrogels for Tissue Engineering Applications. ACS Omega, 4(7), 12647–12656. 10.1021/acsomega.9b01302 [PubMed: 31460385]

Swartzlander MD, Barnes CA, Blakney AK, Kaar JL, Kyriakides TR, & Bryant SJ (2015). Linking the foreign body response and protein adsorption to PEG-based hydrogels using proteomics. Biomaterials, 41, 26–36. 10.1016/j.biomaterials.2014.11.026 [PubMed: 25522962]

Tang X, Gu X, Wang Y, Chen X, Ling J, & Yang Y. (2020). Stable antibacterial polysaccharide-based hydrogels as tissue adhesives for wound healing. RSC Advances, 10(29), Article 29. 10.1039/D0RA02017F

Turabee Md. H., Thambi T, & Lee DS (2019). Development of an Injectable Tissue Adhesive Hybrid Hydrogel for Growth Factor-Free Tissue Integration in Advanced Wound Regeneration. ACS Applied Bio Materials, 2(6), 2500–2510. 10.1021/acsabm.9b00204

Tutak W, Sarkar S, Lin-Gibson S, Farooque TM, Jyotsnendu G, Wang D, Kohn J, Bolikal D, & Simon CG (2013). The support of bone marrow stromal cell differentiation by airbrushed nanofiber scaffolds. Biomaterials, 34(10), 2389–2398. 10.1016/j.biomaterials.2012.12.020 [PubMed: 23312903]

Wallace DG, Cruise GM, Rhee WM, Schroeder JA, Prior JJ, Ju J, Maroney M, Duronio J, Ngo MH, Estridge T, & others. (2001). A tissue sealant based on reactive multifunctional polyethylene glycol. Journal of Biomedical Materials Research, 58(5), Article 5.

Wang J, Li Y, Han X, Zhang H, Fan A, Yao X, Tang B, & Zhang X. (2021). Light-Triggered Antibacterial Hydrogels Containing Recombinant Growth Factor for Treatment of Bacterial Infections and Improved Wound Healing. ACS Biomaterials Science & Engineering, 7(4), 1438–1449. 10.1021/acsbiomaterials.0c01588 [PubMed: 33691399]

Wang L, Zhang X, Yang K, Fu YV, Xu T, Li S, Zhang D, Wang L, & Lee C. (2020). A Novel Double-Crosslinking-Double-Network Design for Injectable Hydrogels with Enhanced Tissue Adhesion and Antibacterial Capability for Wound Treatment. Advanced Functional Materials, 30(1), 1904156. 10.1002/adfm.201904156

Wang Liu, Cherng Lin, Chang Hong, Liu Chiu, Hsu, & Chang. (2019). Biological Effects of Chitosan-Based Dressing on Hemostasis Mechanism. Polymers, 11(11), 1906. 10.3390/polym11111906 [PubMed: 31752424]

Wang Z, He X, He T, Zhao J, Wang S, Peng S, Yang D, & Ye L. (2021). Polymer Network Editing of Elastomers for Robust Underwater Adhesion and Tough Bonding to Diverse Surfaces. ACS Applied Materials & Interfaces, 13(30), 36527–36537. 10.1021/acsami.1c09239 [PubMed: 34313126]

Wu K, Yang Q, Zhang L, Xu P, Wu X, Yang H, Zhou H, Lin X, & Yang L. (2023). An injectable curcumin-releasing organohydrogel with non-drying property and high mechanical stability at low-temperature for expedited skin wound care. Journal of Materials Science & Technology, 133, 123–134. 10.1016/j.jmst.2022.06.002

Xia Q, Liu Z, Wang C, Zhang Z, Xu S, & Han CC (2015). A Biodegradable Trilayered Barrier Membrane Composed of Sponge and Electrospun Layers: Hemostasis and Antiadhesion. Biomacromolecules, 16(9), 3083–3092. 10.1021/acs.biomac.5b01099 [PubMed: 26305870]

Xie Z, Paras CB, Weng H, Punnakitikashem P, Su L-C, Vu K, Tang L, Yang J, & Nguyen KT (2013). Dual growth factor releasing multi-functional nanofibers for wound healing. Acta Biomaterialia, 9(12), 9351–9359. 10.1016/j.actbio.2013.07.030 [PubMed: 23917148]

Xuan C, Hao L, Liu X, Zhu Y, Yang H, Ren Y, Wang L, Fujie T, Wu H, Chen Y, Shi X, & Mao C. (2020). Wet-adhesive, haemostatic and antimicrobial bilayered composite nanosheets for sealing and healing soft-tissue bleeding wounds. Biomaterials, 252, 120018. 10.1016/j.biomaterials.2020.120018

Yan T, Cheng F, Wei X, Huang Y, & He J. (2017). Biodegradable collagen sponge reinforced with chitosan/calcium pyrophosphate nanoflowers for rapid hemostasis. Carbohydrate Polymers, 170, 271–280. 10.1016/j.carbpol.2017.04.080 [PubMed: 28521997]

Yang Y, Liu X, Li Y, Wang Y, Bao C, Chen Y, Lin Q, & Zhu L. (2017). A postoperative anti-adhesion barrier based on photoinduced imine-crosslinking hydrogel with tissue-adhesive ability. Acta Biomaterialia, 62, 199–209. 10.1016/j.actbio.2017.08.047 [PubMed: 28867650]

Ying H, Zhou J, Wang M, Su D, Ma Q, Lv G, & Chen J. (2019). In situ formed collagen-hyaluronic acid hydrogel as biomimetic dressing for promoting spontaneous wound healing. Materials Science and Engineering: C, 101, 487–498. 10.1016/j.msec.2019.03.093

Yu J, Wang K, Fan C, Zhao X, Gao J, Jing W, Zhang X, Li J, Li Y, Yang J, & Liu W. (2021). An Ultrasoft Self-Fused Supramolecular Polymer Hydrogel for Completely Preventing Postoperative Tissue Adhesion. Advanced Materials, 33(16), 2008395. 10.1002/adma.202008395

Yu L, Shang X, Chen H, Xiao L, Zhu Y, & Fan J. (2019). A tightly-bonded and flexible mesoporous zeolite-cotton hybrid hemostat. Nature Communications, 10(1), 1932. 10.1038/s41467-019-09849-9

Yuan H, Chen L, & Hong FF (2020). A Biodegradable Antibacterial Nanocomposite Based on Oxidized Bacterial Nanocellulose for Rapid Hemostasis and Wound Healing. ACS Applied Materials & Interfaces, 12(3), 3382–3392. 10.1021/acsami.9b17732 [PubMed: 31880915]

Yuk H, Varela CE, Nabzdyk CS, Mao X, Padera RF, Roche ET, & Zhao X. (2019). Dry double-sided tape for adhesion of wet tissues and devices. Nature, 575(7781), Article 7781. 10.1038/s41586-019-1710-5

Zhang E, Li J, Zhou Y, Che P, Ren B, Qin Z, Ma L, Cui J, Sun H, & Yao F. (2017). Biodegradable and injectable thermoreversible xyloglucan based hydrogel for prevention of postoperative adhesion. Acta Biomaterialia, 55, 420–433. 10.1016/j.actbio.2017.04.003 [PubMed: 28391053]

Zhang H, Zhao T, Duffy P, Dong Y, Annaidh AN, O'Cearbhaill E, & Wang W. (2015). Hydrolytically Degradable Hyperbranched PEG-Polyester Adhesive with Low Swelling and Robust Mechanical Properties. Advanced Healthcare Materials, 4(15), 2260–2268. 10.1002/adhm.201500406 [PubMed: 26346527]

Zhang K, Lv H, Zheng Y, Yao Y, Li X, Yu J, & Ding B. (2021). Nanofibrous hydrogels embedded with phase-change materials: Temperature-responsive dressings for accelerating skin wound healing. Composites Communications, 25, 100752. 10.1016/j.coco.2021.100752

Zhang W, Ji T, Lyon S, Mehta M, Zheng Y, Deng X, Liu A, Shagan A, Mizrahi B, & Kohane DS (2020). Functionalized Multiarmed Polycaprolactones as Biocompatible Tissue Adhesives. ACS Applied Materials & Interfaces, 12(15), 17314–17320. 10.1021/acsami.0c03478 [PubMed: 32227980]

Zhang Z, Wang X, Wang Y, & Hao J. (2018). Rapid-Forming and Self-Healing Agarose-Based Hydrogels for Tissue Adhesives and Potential Wound Dressings. Biomacromolecules, 19(3), 980–988. 10.1021/acs.biomac.7b01764 [PubMed: 29451778]

Zhao X, Liang Y, Huang Y, He J, Han Y, & Guo B. (2020). Physical Double-Network Hydrogel Adhesives with Rapid Shape Adaptability, Fast Self-Healing, Antioxidant and NIR/pH Stimulus-Responsiveness for Multidrug-Resistant Bacterial Infection and Removable Wound Dressing. Advanced Functional Materials, 30(17), 1910748. 10.1002/adfm.201910748

Zhao X, Sun X, Yildirimer L, Lang Q, Lin Z. Y. (William), Zheng R, Zhang Y, Cui W, Annabi N, & Khademhosseini A. (2017). Cell infiltrative hydrogel fibrous scaffolds for accelerated wound healing. Acta Biomaterialia, 49, 66–77. 10.1016/j.actbio.2016.11.017 [PubMed: 27826004]

Zhao X, Wu H, Guo B, Dong R, Qiu Y, & Ma PX (2017). Antibacterial anti-oxidant electroactive injectable hydrogel as self-healing wound dressing with hemostasis and adhesiveness for cutaneous wound healing. Biomaterials, 122, 34–47. 10.1016/j.biomaterials.2017.01.011 [PubMed: 28107663]

Zhou L, Dai C, Fan L, Jiang Y, Liu C, Zhou Z, Guan P, Tian Y, Xing J, Li X, Luo Y, Yu P, Ning C, & Tan G. (2021). Injectable Self-Healing Natural Biopolymer-Based Hydrogel Adhesive with Thermoresponsive Reversible Adhesion for Minimally Invasive Surgery. Advanced Functional Materials, 31(14), 2007457. 10.1002/adfm.202007457

Zhu J, Li F, Wang X, Yu J, & Wu D. (2018). Hyaluronic Acid and Polyethylene Glycol Hybrid Hydrogel Encapsulating Nanogel with Hemostasis and Sustainable Antibacterial Property for Wound Healing. ACS Applied Materials & Interfaces, 10(16), 13304–13316. 10.1021/acsami.7b18927 [PubMed: 29607644]

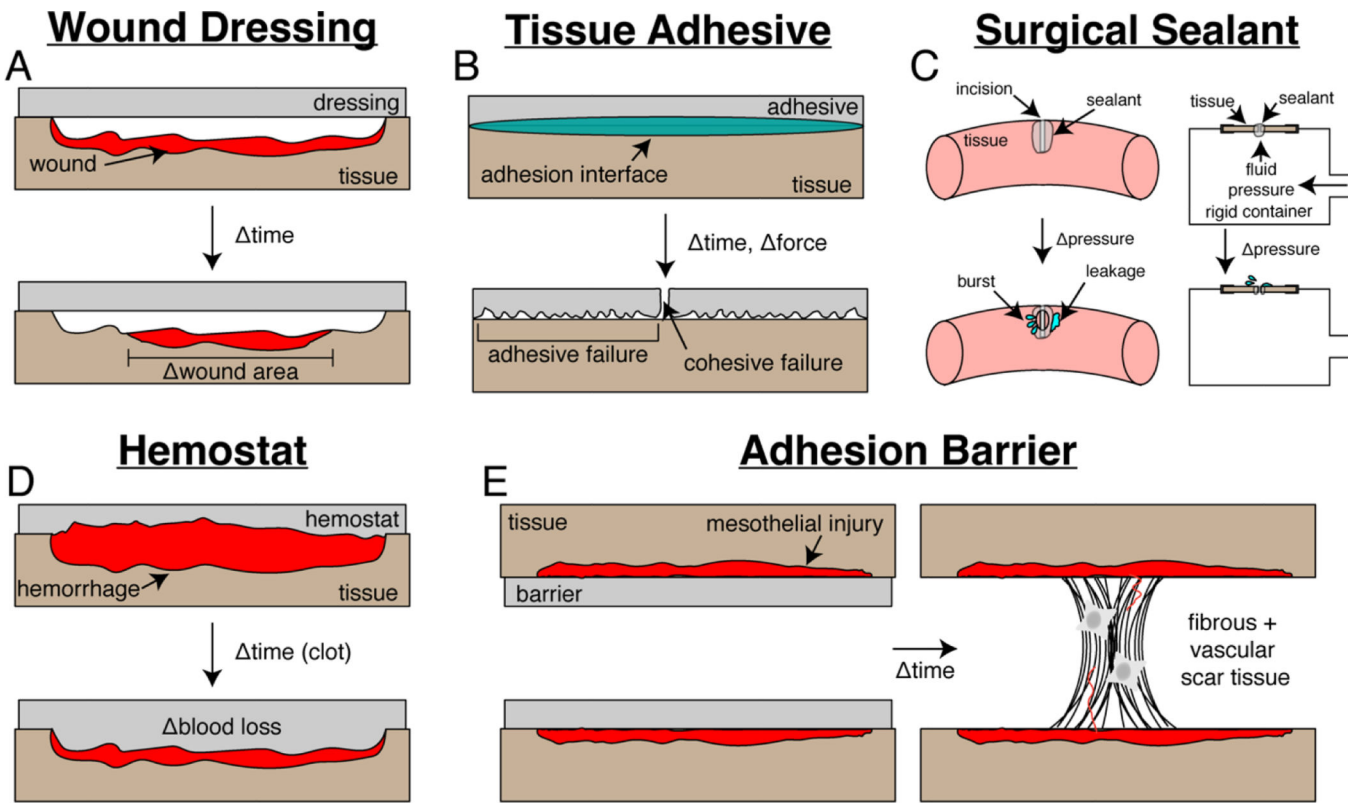

Figure 1:

Schematic of intended function, metrics for clinical assessment, and failure modes for materials deployed in surgery. (a) Wound dressings often encounter minimal shrinkage of damaged tissue as quantified via epidermal wound closure. (b) Tissue adhesives fail due to a combination of bulk and interfacial modes as assessed via adhesion strength. (c) Surgical sealants are ineffective if low burst pressure values are presented in sealing of a defect. (d) Hemostats have limited utility if long clotting times and significant blood loss is encountered. (e) Adhesion barrier failure leads to post-operative scar tissue formation that can be quantified via a scoring rubric.

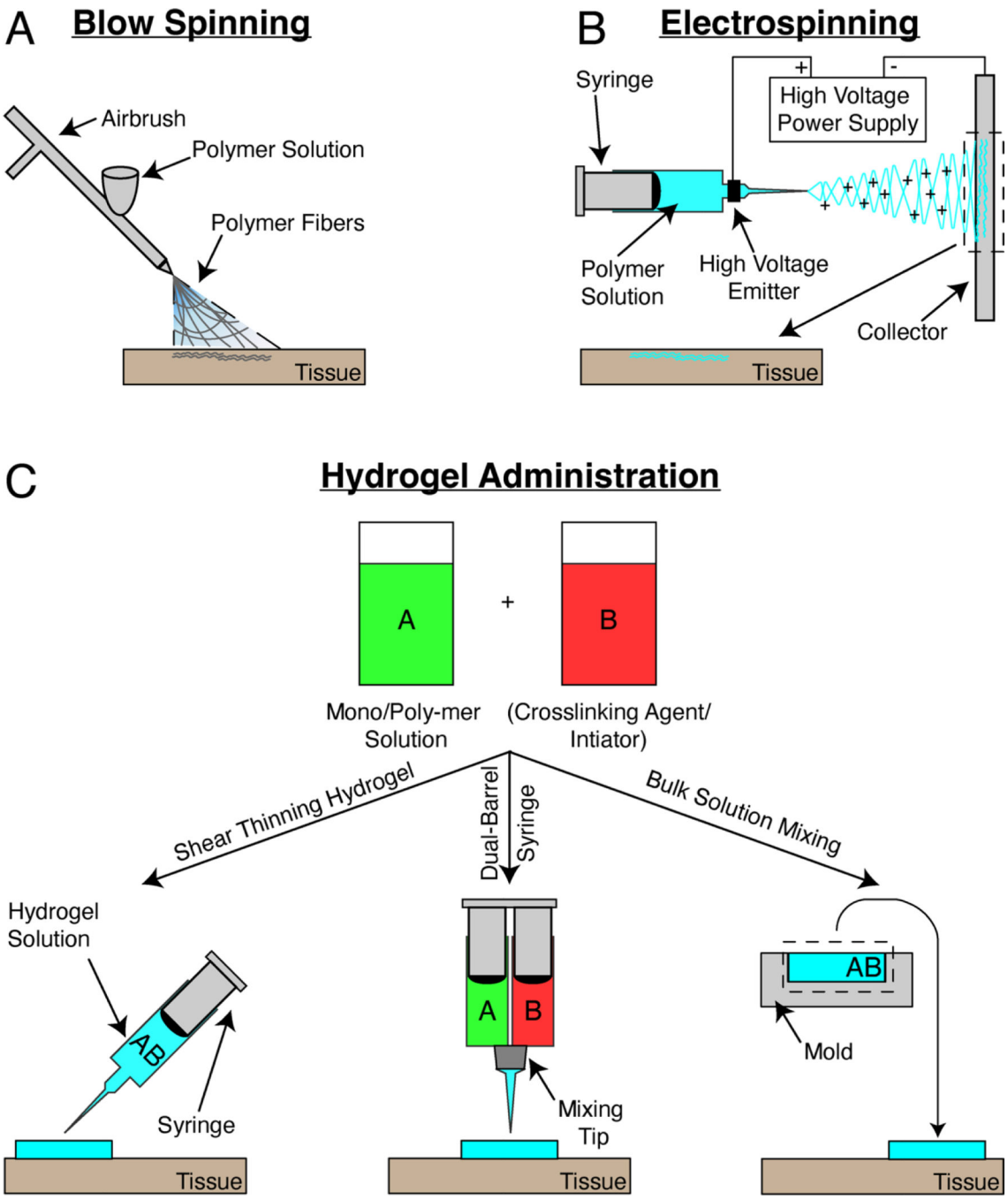

Figure 2:

Schematic of application approaches for nanomaterials used in surgery. (a) Solution blow spinning employs pressure driven flow through a nozzle to generate a collection of fibers with nanoscale diameter and porosity. (b) Electrospinning utilizes a high voltage current and conductive substrate to deposit a nanofiber mat onto a collector and harvested for application to tissue. (c) Hydrogels are synthesized through either combination of a monomer solution with crosslinking agents and initiators or a standalone, neat polymer solution. Injectable hydrogels are ones that display shear thinning behavior and can be injected through a

syringe (left). Non-injectable solutions are either mixed in an attached tip of a dual-barrel syringe (middle) or are mixed as bulk solutions in a mold (right) that are then formed for specific application.

Table 1:

Select fibrous and hydrogel-based nanomaterials employed as wound dressings in surgery.

Composition	Architecture	Mode of Administration	Animal Model, Wound Type	Skin Wound Closure (control vs. test)	Refs.
Poly(lactic-co-glycolic acid) and poly(ethylene glycol)	Fiber	Blowspinning	Pig, partial thickness	100% vs. 80% (t=7d)	(Daristotle, Lau, et al., 2020)
Poly(lactide-co-caprolactone)	Fiber	Blowspinning	Pig, partial thickness	100% vs. 80% (t=7d)	(Daristotle et al., 2021)
Chitosan-poly(vinyl alcohol)-zinc oxide	Fiber	Electrospinning	Rabbit, full thickness	38% vs. 100% (t=12d)	(Ahmed et al., 2018)
L-nitroarginine polyester amide with Pluronic F127 and Tegaderm	Hydrogel	Prefabricated	Rat, full thickness	40% vs. 80% (t=7d)	(M. He et al., 2019)
Chitosan loaded with rose bengal, poly(pyrrole), poly(vinyl alcohol)	Hydrogel	Prefabricated	Rat, partial thickness	15% vs. 40% (t=8d)	(J. Wang et al., 2021)
Poly(vinyl alcohol)/glycerol loaded with curcumin	Hydrogel	Injection	Mouse, full thickness	20% vs. 70% (t=5d)	(Wu et al., 2023)
Gelatin/dopamine	Hydrogel	Injection	Mouse, full thickness	40% vs. 80% (t=7d)	(Y. Huang et al., 2020)
Poly(dopamine)–poly(acrylamide)	Hydrogel	Prefabricated	Mouse, full thickness	10% vs. 50% (t=5d)	(Han, Yan, et al., 2017)

Table 2:

Supplementary fibrous and hydrogel-based nanomaterials employed as wound dressings in surgery.

Composition	Architecture	Mode of Administration	Animal Model, Wound Type	Skin Wound Closure (control vs. test)	Refs.
Chitosan-poly(ethylene oxide)-teicoplanin	Fiber	Electrospinning	Rat, full-thickness	93% vs. 100% (t=14d)	(Amiri et al., 2020)
ECM-related protein Olfactomedinlike	Fiber	Electrospinning	Mouse, full thickness	70% vs. 75% (t=6d)	(Dunn et al., 2016)
Silk fibroin	Fiber	Electrospinning	Rat, full thickness	10% vs. 20% (t=7d)	(Ju et al., 2016)
Chitosan and poly(ethylene oxide) with vascular endothelial growth factor and platelet-derived growth factor	Fiber	Electrospinning	Rat, full thickness	0% vs. 30% (t=7d)	(Xie et al., 2013)
Gelatin methacryloyl with fatty acids/aspirin, encapsulated poly(dopamine)	Hydrogel	Electrospinning	Mouse, full thickness	45% vs. 80% (t=7d)	(K. Zhang et al., 2021)
Gelatin methacryloyl	Fiber	Electrospinning	Mouse, full thickness	60% vs. 80% (t=14d)	(Zhao, Sun, et al., 2017)
Dopamine methacrylamide and sodium tetraborate decahydrate with silver nanoparticles	Hydrogel	Injection	Rat, full thickness	23% vs. 50% (t=10d)	(GhavamiNejad et al., 2016)
Gelatin-grafted-dopamine and poly(dopamine)-coated carbon nanotubes	Hydrogel	Injection	Mouse, full thickness	60% vs. 80% (t=7d)	(Liang, Zhao, Hu, Han, et al., 2019)
Catechol modified methacryloyl chitosan	Hydrogel	Injection	Mouse, full thickness	60% vs. 85% (t=7d)	(L. Wang et al., 2020)
Cross-linked poly(glycerol sebacate)-co-poly(ethylene glycol)-g-catechol and ureido-pyrimidinone modified gelatin	Hydrogel	Injection	Rat, full thickness	95% vs. 100% (t=10d)	(Zhao et al., 2020)
Dopamine-grafted oxidized sodium alginate and poly(acrylamide)	Hydrogel	Prefabricated	Rat, full-thickness	10% vs. 20% (t=5d)	(T. Chen et al., 2018)
Poly(dopamine) nanoparticles with poly (N-isopropylacrylamide) and loaded endothelial growth factor	Hydrogel	Prefabricated	Rat, full thickness	50% vs. 65% (t=9d)	(Han et al., 2016)
Poly(N-isopropyl acrylamide) and alginate with silver nanoparticles	Hydrogel	Prefabricated	Mouse, full-thickness	40% vs. 60% (t=7d)	(Blacklow et al., 2019)
Benzaldehyde-terminated poly(ethylene glycol) and dodecyl-modified chitosan with vascular endothelial growth factor	Hydrogel	Injection	Mouse, full-thickness	60% vs. 80% (t=7d)	(G. Chen et al., 2018)
Methacrylamide dopamine and 2-(dimethylamino)ethyl methacrylate with chitosan	Hydrogel	Injection	Rabbit, full thickness	20% vs. 50% (t=7d)	(Gan et al., 2019)
Multi-armed poly(ethylene glycol)-vinyl sulfone with RGD peptide and FXIIIa coagulant	Hydrogel	Injection	Mouse, full thickness	20% vs. 40% (t=7d)	(Griffin et al., 2015)
N-carboxyethyl chitosan and benzaldehyde-terminated Pluronic F127/carbon nanotubes	Hydrogel	Injection	Injection	70% vs. 85% (t=7d)	(J. He et al., 2020)
Quaternized chitosan-tannic acid-ferric iron	Hydrogel	Injection	Mouse, full thickness	40% vs. 70% (t=7d)	(Guo et al., 2022)

Composition	Architecture	Mode of Administration	Animal Model, Wound Type	Skin Wound Closure (control vs. test)	Refs.
Functionalized quaternized chitosan-gelatin methacrylate-graphene oxide	Hydrogel	Injection	Mouse, full thickness	60% vs. 75% (t=7d)	(Liang et al., 2020)
j-carrageenan polysaccharide loaded with nanosilicates	Hydrogel	Injection	In vitro scratch assay	30% vs. 90% (t=36h)	(Lokhande et al., 2018)
Sodium alginate/graphene oxide/ poly(vinyl alcohol)	Hydrogel	Prefabricated	Mice, full-thickness	65% vs. 70% (t=10d)	(Ma et al., 2019)
Quaternized chitosan and benzaldehyde-terminated Pluronic®F127	Hydrogel	Injection	Mouse, full thickness	80% vs. 90% (t=10d)	(Qu et al., 2018)
Sodium alginate-chitosan-poly(acrylamide)	Hydrogel	Injection	Mouse, full thickness	60% vs. 60% (t=7d)	(Tang et al., 2020)
Collagen-hyaluronic acid	Hydrogel	Injection	Mouse, full thickness	70% vs. 85% (t=7d)	(Ying et al., 2019)
Quaternized chitosan-g-polyaniline and benzaldehyde functionalized poly(ethylene glycol)-co-poly(glycerol sebacate)	Hydrogel	Injection	Mouse, full thickness	80% vs. 85% (t=10d)	(Zhao, Wu, et al., 2017)
Dual-crosslinked chitosan via trans-cyclooctene/tetrazine and four arm poly(ethylene glycol)	Hydrogel	Injection	Mouse, full thickness	62% vs. 85% (t=7d)	(S. Li et al., 2020)
Aminoethyl methacrylate hyaluronic acid and methacrylated methoxy poly(ethylene glycol), chlorhexidine diacetate-loaded nanogels	Hydrogel	Injection	Mouse, full thickness	35% vs. 70% (t=7d)	(Zhu et al., 2018)
Carboxymethyl chitosan and dialdehyde-modified cellulose nanocrystal	Hydrogel	Injection	Mouse, partial thickness	30% vs. 80% (t=7d)	(W. Huang et al., 2018)
Hyaluronic acid-graft-dopamine and reduced graphene oxide	Hydrogel	Injection	Mouse, full thickness	40% vs. 80% (t=7d)	(Liang, Zhao, Hu, Chen, et al., 2019)
Silver/zinc oxide loaded chitosan	Hydrogel	Prefabricated	Mouse, partial thickness	40% vs. 100% (t=7d)	(Lu et al., 2017)
Poly(ε-caprolactone-co-lactide)-b-poly(ethylene glycol)-b-poly(ε-caprolactone-co-lactide) with gelatin	Hydrogel	Injection	Mouse, full thickness	40% vs. 90% (t=7d)	(Turabee et al., 2019)

Table 3:

Select fibrous and hydrogel-based nanomaterials employed as tissue adhesives in surgery.

Composition	Architecture	Mode of Administration	Ex Vivo Tissue Type Used	Adhesion Strength (kPa)	Refs.
Poly(lactide-co-caprolactone)	Fiber	Blowspinning	Pig skin	10	(Daristotle et al., 2021)
Poly(lactide-co-caprolactone)	Fiber	Blowspinning	Pig skin / pig intestine	10 / 10	(Erdi et al., 2022)
Poly(lactide-co-caprolactone)	Fiber	Blowspinning	Pig aorta	30	(Daristotle, Zaki, et al., 2020)
Poly(dopamine) nanoparticles with poly (N-isopropylacrylamide) and loaded endothelial growth factor	Hydrogel	Prefabricated	Pig skin	85	(Han et al., 2016)
Mussel adhesive protein-hyaluronic acid shell with silk fibroin core	Needle patch	Prefabricated	Pig skin / pig intestine	125 / 105	(Jeon et al., 2019)
Four armed poly(ethylene glycol)-N-Hydroxysuccinimide ester	Hydrogel (glue)	Injection	Pig skin	175	(Kelmansky et al., 2017)
Multi armed poly(caprolactone)-N-Hydroxysuccinimide ester	Hydrogel (glue)	Prefabricated	Rat skin	100	(W. Zhang et al., 2020)
Gelatin/chitosan and crosslinked poly(acrylic acid) grafted with N-hydrosuccinimide ester	Hydrogel	Prefabricated	Pig skin / pig intestine / pig aorta	120 / 100 / 100	(Yuk et al., 2019)

Table 4:

Supplementary fibrous and hydrogel-based nanomaterials employed as tissue adhesives in surgery.

Composition	Architecture	Mode of Administration	Ex Vivo Tissue Type Used	Adhesion Strength (kPa)	Refs.
Poly(dopamine)–poly(acrylamide)	Hydrogel	Prefabricated	Human skin (self, in vivo)	17	(Han, Yan, et al., 2017)
Gelatin-grafted-dopamine and poly(dopamine)-coated carbon nanotubes	Hydrogel	Injection	Pig skin	6	(Liang, Zhao, Hu, Han, et al., 2019)
Catechol modified methacryloyl chitosan	Hydrogel	Injection	Pig skin	18	(L. Wang et al., 2020)
Cross-linked poly(glycerol sebacate)-co-poly(ethylene glycol)-g-catechol and ureido-pyrimidinone modified gelatin	Hydrogel	Injection	Pig skin	5	(Zhao et al., 2020)
Dopamine-grafted oxidized sodium alginate and poly(acrylamide)	Hydrogel	Prefabricated	Pig skin	6	(T. Chen et al., 2018)
N-carboxyethyl chitosan and benzaldehyde-terminated Pluronic F127/ carbon nanotubes	Hydrogel	Injection	Pig skin	8	(J. He et al., 2020)
Quaternized chitosan-tannic acid-ferric iron	Hydrogel	Injection	Pig skin	70	(Guo et al., 2022)
Quaternized chitosan and benzaldehyde-terminated Pluronic®F127	Hydrogel	Injection	Pig skin	6	(Qu et al., 2018)
Sodium alginate-chitosan-poly(acrylamide)	Hydrogel	Injection	Pig skin	15	(Tang et al., 2020)
Quaternized chitosan-g-polyaniline and benzaldehyde functionalized poly(ethylene glycol)-co-poly(glycerol sebacate)	Hydrogel	Injection	Pig skin	5	(Zhao, Wu, et al., 2017)
Dual-crosslinked chitosan via trans-cyclooctene/tetrazine and four armed poly(ethylene glycol)	Hydrogel	Injection	Pig skin	16	(S. Li et al., 2020)
Hyaluronic acid-graft-dopamine and reduced graphene oxide	Hydrogel	Injection	Pig skin	5	(Liang, Zhao, Hu, Chen, et al., 2019)
Poly(ε-caprolactone-co-lactide)-b-poly(ethylene glycol)-b-poly(ε-caprolactone-co-lactide) with gelatin	Hydrogel	Injection	Rat skin	100	(Turabee et al., 2019)
Poly(γ-glutamic acid) and dopamine	Hydrogel	Injection	Pig skin	50	(W. Chen et al., 2017)
Dopamine conjugated gelatin macromer	Hydrogel	Prefabricated	Pig skin	25	(Fan et al., 2016)
Poly(dopamine)−chondroitin sulfate−poly(acrylamide)	Hydrogel	Prefabricated	Pig skin	20	(Han et al., 2018)
Poly(acrylic acid)−poly(acrylamide)−poly(dopamine) with poly(N-isopropylacrylamide)	Hydrogel	Prefabricated	Hog skin	12	(X. He et al., 2019)
Dopamine-modified four-armed poly(ethylene glycol) with Laponite nanosilicate	Hydrogel	Injection	Pig aorta	8	(Y. Liu et al., 2014)
Poly(ethylene glycol) diacrylate with dopamine and silica nanoparticles	Hydrogel	Prefabricated	Cow aorta	4.5	(Pinnaratip et al., 2018)
Quaternized chitosan-poly(dopamine)	Hydrogel	Prefabricated	Mice liver	24	(M. Li et al., 2020)
Poly(dopamine)−sodium alginate−polyacrylamide	Hydrogel	Prefabricated	Pig skin	25	(Suneetha et al., 2019)

Composition	Architecture	Mode of Administration	Ex Vivo Tissue Type Used	Adhesion Strength (kPa)	Refs.
Hyperbranched poly(ethylene glycol)-poly(ester)	Hydrogel	Prefabricated	Pig skin / pig aorta	40 / 60	(H. Zhang et al., 2015)
Eight arm poly(ethylene glycol)-N-hydrosuccinimide ester and tannic acid	Hydrogel	Injection	Pig skin	50	(Sun et al., 2020)
Four arm poly(ethylene glycol)-N-hydrosuccinimide ester	Hydrogel	Injection	Pig skin	20	(Bu et al., 2019)
Poly(glycerol sebacate)-acrylate and alginate nanoparticles	Hydrogel (glue)	Injection	Pig aorta	15	(Y. Lee et al., 2015)
Poly(allylamine)−hydrocaffeic acid with catechol and Laponite	Hydrogel	Injection	Pig skin	17	(J. N. Lee et al., 2021)
Poly(glycerol sebacate acrylate)	Hydrogel	Prefabricated	Cow aorta / pig intestine	12.5 / 10	(Lang et al., 2014)
Corticosteroid-modified gelatin particles	Particle suspension	Dropwise	Pig intestine	8	(Nishiguchi & Taguchi, 2020)
Hydroxyapatite with poly(dimethylacrylamide)	Hydrogel	Prefabricated	Mouse skin	42	(Okada et al., 2017)
Antimicrobial peptide in gelatin methacryloyl	Hydrogel	Injection	Pig gingiva	55	(Shirzaei Sani, Portillo Lara, et al., 2019)
Gelatin	Hydrogel	Prefabricated	Pig skin	90	(Shirzaei Sani, Kheirkhah, et al., 2019)
Poly(diolcitrate) with poly(methyl methacrylate)	Hydrogel	Prefabricated	Pig skin	70	(Z. Wang et al., 2021)
Gelatin and chondroitin sulfate	Hydrogel	Injection	Pig skin	30	(Zhou et al., 2021)
Methacryloyl-substituted tropoelastin	Hydrogel	Prefabricated	Pig skin / rat artery	75 / 60	(Annabi et al., 2017)
Poly(acrylamide-methyl acrylate-acrylic acid)	Hydrogel	Prefabricated	Pig intestine	8	(Anthis et al., 2021)
Gelatin methacryloyl	Hydrogel	Injection	Pig skin	45	(Assmann et al., 2017)
Hydrocaffeic acid-modified chitosan with chitosan lactate	Hydrogel	Injection	Pig skin	8	(Du et al., 2020)
Gelatin methacryloyl with N-(2-aminoethyl)−4-(4-(hydroxymethyl)−2-methoxy-5-nitrosophenoxy) butanamide with hyaluronic acid	Hydrogel	Injection	Pig intestine	40	(Hong et al., 2019)
3,4-dihydroxy-L-phenylalanine and hyaluronic acid	Hydrogel	Injection	Pig skin / rat bladder	120 / 140	(H. J. Kim et al., 2015)
Silk fibroin with tannic acid	Hydrogel	Prefabricated	Pig skin / pig aorta	125 / 85	(Bai et al., 2019)

Table 5:

Select fibrous and hydrogel-based nanomaterials employed as surgical sealants.

Composition	Architecture	Mode of Administration	Ex Vivo Tissue Type Used	Burst Pressure (kPa)	Refs.
Poly(lactide-co-caprolactone)	Fiber	Blowspinning	Pig intestine	40	(Daristotle, Zaki, et al., 2020)
Poly(lactic-co-glycolic acid)/ poly(ethylene glycol)	Fiber	Blowspinning	Mouse intestine	9	(Behrens et al., 2015; Kern et al., 2017)
Poly(lactic-co-glycolic acid)/ poly(ethylene glycol)/silica	Fiber	Blowspinning	Pig intestine	19	(Daristotle et al., 2019)
Chitosan film with transglutaminase enzyme	Film	Prefabricated	Collagen membrane / pig intestine	7 / 125	(Fernandez et al., 2017)
Gelatin	Hydrogel	Prefabricated	Pig intestine	60	(Shirzaei Sani, Kheirkhah, et al., 2019)
Gelatin and chondroitin sulfate	Hydrogel	Injection	Pig skin	35	(Zhou et al., 2021)
Four arm poly(ethylene glycol)-N-hydrosuccinimide ester	Hydrogel (glue)	Injection	Pig vein	40	(Bu et al., 2019)
Gelatin methacryloyl with N-(2-aminoethyl)−4-(4-(hydroxymethyl)−2-methoxy-5-nitrosophenoxy) butanamide with hyaluronic acid	Hydrogel	Injection	Pig intestine	40	(Hong et al., 2019)

Table 6:

Supplementary fibrous and hydrogel-based nanomaterials employed as surgical sealants.

Composition	Architecture	Mode of Administration	Ex Vivo Tissue Type Used	Burst Pressure (kPa)	Refs.
Hydrocaffeic acid-modified chitosan with chitosan lactate	Hydrogel	Injection	Pig intestine	10	(Du et al., 2020)
Chitosan-catechol	Film	Prefabricated	Rat intestine	27	(Ryu et al., 2019)
Gelatin methacryloyl	Hydrogel	Injection	Collagen membrane / rat lung	15 / 6	(Assmann et al., 2017)
Hyaluronic acid/gelatin	Hydrogel	Injection	Dog intestine	20	(Luo et al., 2019)
Four arm poly(ethylene glycol)-N-hydrosuccinimide ester	Hydrogel	Injection	Collagen membrane	9	(Kelmansky et al., 2017)
Eight arm poly(ethylene glycol)-N-hydrosuccinimide ester and tannic acid	Hydrogel	Injection	Pig artery	24	(Sun et al., 2020)
Four armed poly(ethylene glycol)-poly(lactic-co-glycolic acid)-N-Hydroxysuccinimide ester	Hydrogel (glue)	Injection	Collagen membrane	13	(Shimony et al., 2021)
Mussel adhesive protein-hyaluronic acid shell with silk fibroin core	Needle patch	Prefabricated	Pig intestine	13	(Jeon et al., 2019)
Methacryloyl-substituted tropoelastin	Hydrogel	Prefabricated	Collagen membrane / rat lung / pig lung	12 / 6 / 3	(Annabi et al., 2017)
Poly(acrylamide-methyl acrylate-acrylic acid)	Hydrogel	Prefabricated	Pig intestine	13	(Anthis et al., 2021)
Agarose−ethylenediamine conjugate and dialdehyde-functionalized poly(ethylene glycol)	Hydrogel	Prefabricated	Pig skin	16	(Z. Zhang et al., 2018)

Table 7:

Select fibrous and hydrogel-based nanomaterials deployed as hemostats in surgery.

Composition	Architecture	Mode of Administration	Animal Model - Blood Loss	Blood Loss (control vs. test)	Clotting Time - Model	Clotting Time (control vs. test)	Refs.
N-(3-aminopropyl)methacrylamide	Hydrogel particles	Prefabricated	Rat liver puncture / rat tail amputation	500 mg vs. 200 mg / 3 g vs. 500 mg	Rat liver puncture / rat tail amputation	1.5 min vs. 0.25 min / 18 min vs. 5 min	(Behrens et al., 2014)
Zeolite-loaded alginate-chitosan	Hydrogel particles	Prefabricated	N/A	N/A	In vitro whole blood	9 min vs. 15 s	(Fathi et al., 2018)
Poly(lactic-co-glycolic acid)/ poly(ethylene glycol)/silica	Fiber	Blowspinning	N/A	N/A	Pig liver laceration	4 min vs. 3 min	(Daristotle et al., 2019)
Quaternized chitosan-poly(dopamine)	Hydrogel	Prefabricated	Mouse tail amputation / mouse liver prick / rat liver incision / rabbit liver resection / pig skin laceration	125 mg vs. 10 mg / 500 mg vs. 20 mg / 960 mg vs. 30 mg / 10 g vs. 1 g / 400 mg vs. 30 mg	Mouse tail amputation / mouse liver prick / rat liver incision / rabbit liver resection / pig skin laceration	545 s vs. 80 s / 316 s vs. 20 s / 204 s vs. 60 s / 425 s vs. 200 s / 200 s vs. 50 s	(M. Li et al., 2020)
Dopamine and antimicrobial peptide modified gelatin methacryloyl with poly(caprolactone) layer	Film	Prefabricated	Mouse skin biopsy / rat liver incision	275 mg vs. 10 mg / 440 mg vs. 50 mg	Mouse skin biopsy / rat liver incision	450 s vs. 200 s / 330 s vs. 60 s	(Xuan et al., 2020)
Silk fibroin with tannic acid	Hydrogel	Prefabricated	Rat liver puncture	425 mg vs. 40 mg	In vitro whole blood	5.5 min vs. 1 min	(Bai et al., 2019)
Agarose−ethylenediamine conjugate and dialdehyde-functionalized poly(ethylene glycol)	Hydrogel	Prefabricated	Rabbit liver incision	700 mg vs. 200 mg	Rabbit liver incision	75 s vs. 10 s	(Z. Zhang et al., 2018)
Chitosan/gelatin composite sponge	Foam	Prefabricated	Rabbit liver puncture / rabbit ear artery puncture	17 g vs. 4 g / 3 g vs. 1 g	Rabbit liver puncture / rabbit ear artery puncture	100 s vs. 40 s / 100 s vs. 50 s	(Lan et al., 2015)
Poly(dextran aldehyde)	Foam	Prefabricated	Rabbit liver incision / rabbit ear artery incision / rabbit femoral artery incision	1.1 g vs. 0.3g / 7.5 g vs. 0.1 g / 8 g vs. 0.1 g	Rabbit liver incision / rabbit ear artery incision / rabbit femoral artery incision	420 s vs. 240 s / 250 s vs. 50 s / 180 s vs. 120 s	(C. Liu et al., 2019)

Table 8:

Supplementary fibrous and hydrogel-based nanomaterials deployed as hemostats in surgery.

Composition	Architecture	Mode of Administration	Animal Model - Blood Loss	Blood Loss (control vs. test)	Clotting Time - Model	Clotting Time (control vs. test)	Refs.
Poly(diolcitrate) with poly(methyl methacrylate)	Hydrogel	Prefabricated	Rat liver puncture	500 mg vs. 200 mg	N/A	N/A	(Z. Wang et al., 2021)
Hydrocaffeic acid-modified chitosan with chitosan lactate	Hydrogel	Injection	Rat liver incision	375 mg vs. 20 mg	Rat liver incision	120 s vs. 30 s	(Du et al., 2020)
Gelatin methacryloyl with N-(2-aminoethyl) −4-(4-(hydroxymethyl) −2-methoxy-5-nitrosophenoxy) butanamide with hyaluronic acid	Hydrogel	Injection	Rabbit liver resection	220 mg vs. 90 mg	N/A	N/A	(Hong et al., 2019)
Hyaluronic acid/gelatin	Hydrogel	Injection	Rat liver incision	240 mg vs. 100 mg	N/A	N/A	(Luo et al., 2019)
Poly(2-hydroxyethyl methacrylate)-methacrylic acid N-hydroxysuccinimide ester-fluorescein methacrylate with transglutaminase factor XIIIa	Suspension	Dropwise	N/A	N/A	Rat artery catheter	1 min vs. 0.75 min	(Chan et al., 2015)
RADA16-I peptide with hyaluronic acid coated gauze	Film	Prefabricated	N/A	N/A	Pig skin 8 mm biopsy	5 min vs. 2 min	(Hsu et al., 2015)
N-(2-hydroxypropyl)-3-trimethylammonium chitosan chloride and poly(dextran aldehyde)	Hydrogel	Injection	Rat liver puncture	170 mg vs. 45 mg	N/A	N/A	(Hoque et al., 2017)
Starch-based hydrogel	Hydrogel	Injection	Rat femoral artery incision	7 g vs. 2g	N/A	N/A	(Mao et al., 2021)
Silica nanoparticle coated with poly(dopamine)	Particle suspension	Dropwise	Rat femoral artery incision / rat liver incision	4.5 g vs. 1.25 g / 1 g vs. 0.2 g	Rat femoral artery incision / rat liver incision	250 s vs. 170 s / 120 s vs. 100 s / 140 s vs. 80 s	(C. Liu et al., 2018)
Hydrophobically modified chitosan	Foam	Aerosol spray	Rat liver resection	28 mL vs. 9 mL	N/A	N/A	(Dowling et al., 2015)
Collagen sponge with chitosan/calcium pyrophosphate	Foam	Prefabricated	Rabbit artery incision / rat liver resection	1.6 g vs. 1 g / 1.5 g vs. 1 g	Rabbit artery incision / rat liver resection	164 s vs. 135 s / 184 s vs. 106 s	(Yan et al., 2017)
Poly(caprolactone) foam coated with gelatin	Foam	Electrospinning	N/A	N/A	In vitro human whole blood	100 s vs. 20 s	(S. Chen et al., 2018)
Cellulose and chitosan with collagen	Foam	Prefabricated	Rat liver resection	140 mg vs. 60 mg	Rat liver resection	180 s vs. 90 s	(Yuan et al., 2020)
Zeolite chabazite on the cotton fiber surface	Fiber	Prefabricated	Rabbit femoral	10 g vs. 7 g	Rabbit femoral	400 s vs. 150 s	(L. Yu et al., 2019)

Composition	Architecture	Mode of Administration	Animal Model - Blood Loss	Blood Loss (control vs. test)	Clotting Time - Model	Clotting Time (control vs. test)	Refs.
			artery incision		artery incision		

Table 9:

Select fibrous and hydrogel-based nanomaterials deployed as adhesion barriers in surgery.

Composition	Architecture	Mode of Administration	Animal Model (Evaluation Time Point)	Adhesion Score (control vs. test) (Scale)	Refs.
Poly(lactide-co-caprolactone)	Fiber	Blowspinning	Mouse cecal ligation (t=7d)	3.5 vs. 2.5 (0 to 5)	(Erdi et al., 2022)
Poly(ethylene glycol)/ poly(caprolactone)	Fiber	Electrospinning	Rabbit tendon anastomosis (t=14d)	3.5 vs. 1 (0 to 5)	(C.-H. Chen et al., 2015)
Dodecyl-modified hydroxypropyl methylcellulose with poly(ethylene glycol)-b-poly(lactic acid)	Hydrogel	Injection	Rat cardiac infarct (t=28d) / Rat abdominal wall ligation (t=28d)	4.2 vs. 0.6 (0 to 5) / 3.2 vs. 1.35 (0 to 5)	(Stapleton et al., 2019, 2021)
N,Ocarboxymethyl chitosan and aldehyde hyaluronic acid	Hydrogel	Injection	Rat abdominal wall abrasion (t=7d)	5 vs. 0.3 (0 to 5)	(Song et al., 2016)
Poly(ethylene glycol)-block-poly(L-lactide-co-glycolide) with 10-hydroxycamptothecin and diclofenac sodium drugs	Fiber	Electrospinning	Mouse cecal abrasion (t=14d)	2.9 vs. 0.3 (0 to 4)	(J. Li et al., 2018)
Celecoxib-loaded poly(L-lactic acid)-poly(ethylene glycol) and hyaluronic acid	Fiber	Electrospinning	Rabbit tendon anastomosis (t=21d)	4 vs. 1.75 (0 to 5)	(Jiang et al., 2015)

Table 10:

Supplementary fibrous and hydrogel-based nanomaterials deployed as adhesion barriers in surgery.

Composition	Architecture	Mode of Administration	Animal Model (Evaluation Time Point)	Adhesion Score (control vs. test) (Scale)	Refs.
Squid ring teeth protein coated poly(propylene)	Mesh	Prefabricated	Rat abdominal wall resection (t=7d)	3.1 (0 to 5)	(Leberfinger et al., 2018)
Poly(lactide-co-glycolide)/ poly(lactide)-b-poly(ethylene glycol) fibers with layers of carboxymethyl chitosan sponge	Electrospinning and foam	Electrospinning and prefabricated	Rat abdominal wall abrasion (t=10d)	2.4 vs. 0.23 (0 to 3)	(Xia et al., 2015)
Pullulan hydrogel	Hydrogel	Injection	Mouse cecal abrasion (t=14d)	2.67 vs. 0.5 (0 to 4)	(Bang et al., 2016)
Carboxymethyl chitosan/ carboxymethyl cellulose/collagen	Hydrogel	Prefabricated	Rat cecal abrasion (t=7d)	3 vs. 0.5 (0 to 4)	(Cai et al., 2018)
Poly(N-isopropylacrylamide)grafted to chitosan and conjugated with hyaluronic acid	Hydrogel	Injection	Rat cecal abrasion (t=14d)	3 vs. 0 (0 to 3)	(C.-H. Chen et al., 2017)
Pluronic F127 and oxidized hyaluronic acid	Hydrogel	Injection	Rat cecal abrasion (t=7d)	4.5 vs. 0.33 (0 to 5)	(Z. Li et al., 2020)
Alginate and hyaluronic acid	Hydrogel	Prefabricated	Rat cecal and abdominal wall abrasion (t=14d)	2.5 vs. 0.1 (0 to 3)	(Mayes et al., 2020)
Silicate nanoplatelets and poly(ethylene oxide)	Hydrogel	Injection	Rat abdominal wall ligation (t=14d)	1.25 vs. 0 (0 to 3)	(Ruiz-Esparza et al., 2021)
Hyaluronic acid with phenolic hydroxyl moieties	Hydrogel	Injection	Mouse abdominal wall abrasion (t=7d)	2.8 vs. 0.6 (0 to 3)	(Sakai et al., 2015)
Hyaluronic acid with tempo-oxidized nanocellulose/methyl cellulose/poly(ethylene glycol)	Hydrogel	Injection	Rat cecal abrasion (t=7d)	3.5 vs. 0 (0 to 4)	(Sultana et al., 2020)
Hyaluronic acid with tempo-oxidized nanocellulose/methyl cellulose/poly(ethylene glycol)	Hydrogel	Injection	Rat cecal abrasion (t=7d)	3.875 vs. 0 (0 to 4)	(Sultana et al., 2019)
Carboxymethyl cellulose and glycol chitosan	Hydrogel	Injection	Rat cecal abrasion (t=14d)	4.9 vs. 1.7 (0 to 5)	(Yang et al., 2017)
Poly(N-acryloyl alaninamide)	Hydrogel	Injection	Rat cecal abrasion (t=14d)	4.8 vs. 0.2 (0 to 5)	(J. Yu et al., 2021)
Galactose modified xyloglucan	Hydrogel	Injection	Rat cecal abrasion (t=7d)	4.25 vs. 0.125 (0 to 5)	(E. Zhang et al., 2017)